CYP2J2 metabolites, epoxyeicosatrienoic acids, attenuate Ang II-induced cardiac fibrotic response by targeting Gα$_{12/13}$ [s]

Zuowen He,[*,†] Yong Yang,[*,†] Zheng Wen,[*,†] Chen Chen,[*,†] Xizhen Xu,[*,†] Yanfang Zhu,[*] Yan Wang,[*,†] and Dao Wen Wang[1,*,†]

Division of Cardiology, Department of Internal Medicine, Tongji Hospital, Tongji Medical College* and Hubei Key Laboratory of Genetics and Molecular Mechanisms of Cardiological Disorders,[†] Huazhong University of Science and Technology, Wuhan 430030, People's Republic of China

Abstract The arachidonic acid-cytochrome P450 2J2-epoxyeicosatrienoic acid (AA-CYP2J2-EET) metabolic pathway has been identified to be protective in the cardiovascular system. This study explored the effects of the AA-CYP2J2-EET metabolic pathway on cardiac fibrosis from the perspective of cardiac fibroblasts and underlying mechanisms. In in vivo studies, 8-week-old male CYP2J2 transgenic mice (aMHC-CYP2J2-Tr) and littermates were infused with angiotensin II (Ang II) or saline for 2 weeks. Results showed that CYP2J2 overexpression increased EET production. Meanwhile, impairment of cardiac function and fibrotic response were attenuated by CYP2J2 overexpression. The effects of CYP2J2 were associated with reduced activation of the α subunits of G12 family G proteins (Gα$_{12/13}$)/RhoA/Rho kinase (ROCK) cascade and elevation of the NO/cyclic guanosine monophosphate (cGMP) level in cardiac tissue. In in vitro studies, cardiac fibroblast activation, proliferation, migration, and collagen production induced by Ang II were associated with activation of the Gα$_{12/13}$/RhoA/ROCK pathway, which was inhibited by exogenous 11,12-EET. Moreover, silencing of Gα$_{12/13}$ or RhoA exerted similar effects as 11,12-EET. Furthermore, inhibitory effects of 11,12-EET on Gα$_{12/13}$ were blocked by NO/cGMP pathway inhibitors.[JLR] Our findings indicate that enhancement of the AA-CYP2J2-EET metabolic pathway by CYP2J2 overexpression attenuates Ang II-induced cardiac dysfunction and fibrosis by reducing the fibrotic response of cardiac fibroblasts by targeting the Gα$_{12/13}$/RhoA/ROCK pathway via NO/cGMP signaling.—He, Z., Y. Yang, Z. Wen, C. Chen, X. Xu, Y. Zhu, Y. Wang, and D. W. Wang. **CYP2J2 metabolites, epoxyeicosatrienoic acids, attenuate Ang II-induced cardiac fibrotic response by targeting Gα$_{12/13}$.** *J. Lipid Res.* 2017. **58:** 1338–1353.

Supplementary key words cytochrome P450 2J2 • cardiac fibrosis • cardiac fibroblast • α subunits of G12 family G proteins • angiotensin II

Myocardial fibrosis is an important pathophysiological process occurring with various cardiac injuries and diseases (1). Cardiac fibroblasts have been described to exhibit the earliest, most dramatic, and most sustained proliferative, migratory, and transformational responses to profibrotic factors resulting in cardiac fibrosis (2–4). Arachidonic acid (AA) is a kind of polyunsaturated fatty acid, which has been widely studied in recent years, especially in the cardiovascular field (5). We focused on the cytochrome P450 epoxygenase (CYP450) metabolite pathway, which acts as the third pathway of AA metabolism after the pathway of cyclooxygenase and lipoxygenase (LOX). Epoxyeicosatrienoic acids (EETs) are predominant metabolites of the AA-CYP450 metabolic pathway and are primarily generated by cytochrome P450 2J2 (CYP2J2) in human heart (6). The AA-CYP2J2-EET pathway has been widely studied in recent years and has been shown to play multiple biological roles in cardiovascular homeostasis (6–10). Previous research has demonstrated that a polymorphism of CYP2J2 is significantly associated with coronary artery disease and the risk of ischemic stroke (11, 12). Additionally, pharmacological and genetic manipulations of CYP450 and soluble epoxide hydrolase (sEH) with changed EET levels have demonstrated contributions for the AA-CYP450-EET-sEH

metabolic pathway to cardiovascular diseases, given the impact of EETs to cardiovascular physiology (6–10). Our previous works have demonstrated protective effects of the AA-CYP2J2-EET metabolic pathway from the perspective of cardiomyocytes and cellular cross-talk (8, 13–15). However, the role of the AA-CYP2J2-EET system on cardiac fibrosis and fibroblasts has not been completely elucidated. Therefore, this study focused on the role of the AA-CYP2J2-EET metabolic pathway in cardiac fibrosis from the perspective of cardiac fibroblasts and the underlying mechanisms involved in this process.

Previous research has excluded the competitive binding ability of EETs to angiotensin II (Ang II) type I receptor (AT1R) for the reason that neither EET nor dihydroxyeicosatrienoic acid (DHET) showed any appreciable affinity for AT1Rs (16). Increasing evidence from experimental animal models and humans indicates that α subunits of G12 family G proteins ($G\alpha_{12/13}$) activity is increased in the failing heart and its activation contributes to the pathogenesis of myocardial fibrosis (17, 18). Recent progress toward understanding the mechanisms of cardiac fibrosis has revealed that $G\alpha_{12/13}$ activation plays a pivotal role in regulating the phenotype of cardiac fibroblasts (19, 20), while it also acts as a key determinant of the migration and growth of various types of cells (21–23). All of these factors contribute to collagen accumulation in cardiac tissue. The profibrotic effects of $G\alpha_{12/13}$ have been shown to be mainly mediated by RhoA and subsequent Rho kinase (ROCK) activation (24, 25). Therefore, we investigated the role of the AA-CYP2J2-EET metabolic pathway on $G\alpha_{12/13}$ and its effectors RhoA/ROCK cascade in cardiac fibroblasts. As eNOS and NO release, which is induced by EETs (26–28), can inhibit the activation of $G\alpha_{12/13}$ (29), we postulated that EETs might attenuate fibrotic response by inhibiting the $G\alpha_{12/13}$/RhoA/ROCK pathway via NO/cyclic guanosine monophosphate (cGMP) activation. This hypothesis will be confirmed in vivo and in vitro in mice exhibiting cardiomyocyte-specific expression of CYP2J2 and primary cardiac fibroblast cultures, respectively.

MATERIALS AND METHODS

Animal experiment

Mice with cardiomyocyte-specific expression of CYP2J2 were kindly gifted by Dr. Zeldin's laboratory (National Institute of Environmental Health Sciences), and transgenic mice were genotyped as described previously (30). All experimental procedures were approved by the Experimental Animal Research Committee of Tongji Medical College, Huazhong University of Science and Technology, and were in strict accordance with the *Guide for the Care and Use of Laboratory Animals* published by the US National Institutes of Health (NIH Publication No. 85-23, revised 1996) and the Public Health Service Policy on Humane Care and Use of Laboratory Animals.

Eight-week-old male CYP2J2 transgenic mice and age-/sex-matched littermates breeding from the heterozygous CYP2J2-transgenic mice were anesthetized by an intraperitoneal injection of a mixture of xylazine (5 mg/kg) and ketamine (80 mg/kg) and then osmotic mini-pumps (Alzet model 1002; Alza) containing saline or Ang II (Sigma-Aldrich, St. Louis, MO) (n = 10 per group)

were implanted subcutaneously for 2 weeks. The infusion rate of Ang II or saline was 1.5 μg/kg/min. Two weeks later, the mice were euthanized with carbon dioxide and tissues were collected for various experiments.

Hemodynamic measurements and echocardiography

Echocardiographic examination was performed by using an echocardiography system with a 30 MHz high-frequency scan head (VisualSonicsVevo770; VisualSonics Inc., Toronto, Canada) under light (1–2%) isoflurane anesthesia, as previously described (31). Left ventricle hemodynamic measurements were performed by using a Millar catheter system through the left carotid artery under intraperitoneal injection of 90 mg/kg ketamine and 10 mg/kg xylazine, as described previously (32).

Neonatal rat cardiac fibroblast isolation and cultures

Cardiac fibroblasts were isolated and cultured as described previously (33, 34). Briefly, hearts were excised from 1- to 2-day-old rats after 4–5% isoflurane inhalation anesthesia. Hearts were minced and digested in 0.06% (w/v) trypsin (Invitrogen, Life Technologies Corporation, Carlsbad, CA) and 0.025% (w/v) collagenase type II (Invitrogen, Life Technologies Corporation) in calcium-free Hanks' buffer (with HEPES) by serial digestion. Cells were centrifuged and resuspended in Dulbecco's modified Eagle's medium:F12 medium (Invitrogen, Life Technologies Corporation) with 10% (v/v) fetal calf serum and 1% penicillin/streptomycin (Invitrogen, Life Technologies Corporation). Cardiac fibroblasts were separated from cardiomyocytes by differential adhesion. The attached cardiac fibroblasts were subsequently cultured with Dulbecco's modified Eagle's medium:F12 medium (Invitrogen, Life Technologies Corporation) with 10% (v/v) fetal calf serum and 1% penicillin/streptomycin. Cardiac fibroblasts grew robustly and were confluent in 4–6 days and the cells were passed once to eliminate any myocytes that adhered during the incubation. The second to fifth passages of cardiac fibroblasts were used for the following experiments.

Treatments of cardiac fibroblasts. In treatment 1, cardiac fibroblasts (3×10^5 cells per well) were serum-starved overnight and then incubated with or without Ang II (1 μM) in the presence or absence of 11,12-EET (1 μM; Cayman Chemical, Ann Arbor, MI) or 14,15-EEZE (1 μM) for 5 min, 6 h, or 24 h. In treatment 2, transfections with $G\alpha_{12}$ siRNA, $G\alpha_{13}$ siRNA, RhoA siRNA, and control siRNA (100 nM; RiboBio, Guangzhou, China) were performed with Lipofectamine 2000 reagent (Invitrogen, Life Technologies Corporation) for 48 h and then the cells were incubated with or without Ang II or 11,12-EET for 5 min, 6 h, or 24 h, respectively. In treatment 3, cardiac fibroblasts (3×10^5 cells per well) were serum-starved overnight and then incubated with or without Ang II (1 μM) in the presence or absence of 11,12-EET, 1H-[1,2,4]oxadiazolo[4,3-a]quinoxalin-1-one (10 μM; Sigma-Aldrich), hydroxocobalamin (200 μM; Sigma-Aldrich), or L-N^5-(1-iminoethyl)ornithine hydrochloride (100 μM; Sigma-Aldrich) for 5 min.

The cells that were incubated with various reagents for 5 min were used for $G\alpha_{12/13}$/RhoA/ROCK cascade detection; the cells that were incubated with various reagents for 6 h were used for migration detection; and the cells that were incubated with various reagents for 24 h were used for Western blots and immunofluorescence.

Neonatal mouse cardiomyocyte isolation and cultures

Neonatal cardiomyocytes from WT mice or transgenic mice were isolated as described previously (35). Cells were incubated with saline or Ang II (1 μmol/l) for 6 h, after overnight serum-starvation,

and then cultured medium was collected for eicosanoid detection. The detailed experimental process is described in the supplemental data.

Histological analysis

Heart sections were stained with α-smooth muscle actin (α-SMA) (Abcam, Cambridge, MA) and picrosirius red (Sigma-Aldrich) as previously described (36).

Western blotting analysis

Western blots were performed to detect expression of various proteins. Quantity One software was used for band analysis (Bio-Rad, Hercules, CA).

Immunofluorescence

Immunofluorescent staining for α-SMA and proliferating cell nuclear antigen (PCNA) (Proteintech, Wuhan, China) was performed as described previously (37).

Plasmid constructions

cDNAs encoding the regulatory tetratricopeptide repeat domain (TPR) of Ser/Thr protein phosphatase type 5 (PP5-TPR) with *Bam*HI and *Eco*RI sites were generated by PCR from mouse cDNA using the primers, 5′-CGGGATCCGAGTGTGCTGAGACCCCCC-3′ and 5′-CGGAATTCATCTTGGCATCCTTGTCATTAG-3′, and subcloned into *Bam*HI/*Eco*RI sites of the PGEX-6p-1 vector, respectively.

Recombinant protein expression

Recombinant proteins were expressed as glutathione *S*-transferase (GST)-TPR fusion proteins in BL21 (DE3) pLysS chemically competent cells (Transgene Biotek) and purified on glutathione-Sepharose beads according to the method of Amano et al. (38).

RhoA activity assay

RhoA activity was detected as described previously (29). Briefly, cardiac fibroblasts treated with various reagents were lysed with an ice-cold cell lysis buffer [10 mM $MgCl_2$, 25 mM HEPES (pH 7.5), 10% glycerol, 150 mM NaCl, 1 mM EDTA, and 1% Igepal CA-630]. Cell lysates were incubated with glutathione-Sepharose beads (Cytoskeleton, Inc.), which were bound to the GST-fused Rho-binding domain of Rhotekin (GST-RBD) for 1 h at 4°C, and bound proteins were immunoblotted with anti-RhoA antibodies. Detailed protocols for RhoA activity detection are presented in the supplemental Methods.

$G\alpha_{12/13}$ activity assay

$G\alpha_{12/13}$ activity was detected as described previously (29). Briefly, cardiac fibroblasts treated with various reagents were lysed with ice-cold cell lysis buffer [20 mM HEPES, 0.1% Triton X-100 (pH 8.0), 2 mM $MgCl_2$, 1 mM EDTA, 10 g/ml aprotinin, 1 mM phenylmethylsulfonyl fluoride, and 10 g/ml leupeptin]. Cell lysates were then incubated with glutathione-Sepharose beads, which were bound to GST-TPR fusion protein for 2 h at 4°C. The bound proteins were immunoblotted with anti-G12 and anti-G13 antibodies. Detailed protocols for $G\alpha_{12/13}$ activity detection are presented in supplemental Methods.

Determination of NO concentrations

NO concentrations were detected as described previously (26). Samples were analyzed for NO (nitrate and nitrite) concentrations by using nitrate/nitrite fluorometric assay kits (Cayman Chemical). NO concentrations were normalized to the protein content. A detailed protocol for the detection of NO is presented in supplemental Methods.

cGMP measurements

Cardiac tissue cGMP and intracellular cGMP were determined by enzyme immunoassay kits (Cayman Chemical) following the manufacturer's instructions. A detailed protocol for cGMP detection is presented in the supplemental Methods.

Transwell analysis

Transwell Boyden chambers (24-well insert, 8.0 μm; BD Biosciences) were used to determine the migration of cardiac fibroblasts, as described previously (39). Cells were pretreated with various reagents, and then 1×10^5 cells were seeded in the top chamber with noncoated membranes. Cells were then seeded in a serum-free medium migrated toward medium incubated with Ang II. Cells that migrated to the lower surface of the filters were counted in five random high-power fields.

Eicosanoid detection

Eicosanoids were measured by LC/MS/MS following the established method described previously (40, 41). Detailed information, including the sample preparation, LC/MS/MS conditions, and precision and accuracy of this method are described in the supplemental Methods.

Statistical analysis

All data are expressed as mean ± SEM. The in vivo data were analyzed using paired *t*-test and one-way ANOVA. The in vitro data were analyzed by one-sample *t*-test and one-way ANOVA. Statistical significance was defined as $P < 0.05$.

RESULTS

Cardiomyocyte-specific expression of CYP2J2 enhances production of EETs

LC/MS/MS results showed that concentrations of all four EETs in cardiac tissue were increased in transgenic mice compared with WT mice under the saline-infused condition (**Table 1**). Ang II infusion reduced concentrations of all four EETs in cardiac tissue of WT mice compared with the saline-WT group, but did not affect concentrations of EETs in cardiac tissue of transgenic mice (Table 1). Similar results were observed in plasma and cardiomyocyte cultured medium (Tables 1, **2**, and **3**). As EETs are further converted to more stable and less bioactive metabolites, DHETs (42), this leads to increased concentrations of DHETs in cardiac tissue, plasma, and cultured medium in CYP2J2 transgenic mice (Tables 1–3). Therefore, we performed additional experiments to detect whether DHETs affect cardiac fibroblasts. Results showed that collagen type I (COL I) and α-SMA upregulation induced by Ang II were not attenuated by 11,12-DHET from 0.3 to 3 μM (supplemental Fig. S3C, D). Other metabolites were not changed by CYP2J2 overexpression compared with WT mice under both saline- and Ang II-infused conditions (Tables 1–3). We also detected whether 17,18-epoxyeicosatetraenoic acid (EEQ), the predominant epoxide of EPA, could affect cardiac fibrotic response. Results showed that COL I and α-SMA upregulation induced by Ang II (1 μM) were not attenuated by 17,18-EEQ (1 μM) incubation (supplemental Fig. 3A, B). These results revealed that cardiomyocyte-specific expression of CYP2J2 enhanced AA metabolizing

TABLE 1. Eicosanoids levels in cardiac tissue measured by LC/MS/MS

	Saline		Ang II	
	WT	αMHC-CYP2J2-Tr	WT	αMHC-CYP2J2-Tr
AA-CYP epoxygenase				
5,6-EET	51.90 ± 2.33	172.20 ± 6.13^{a}	39.78 ± 2.00^{a}	$160.93 \pm 3.87^{a,b}$
8,9-EET	62.61 ± 2.54	247.40 ± 4.48^{a}	50.34 ± 3.25^{a}	$235.53 \pm 5.40^{a,b}$
11,12-EET	80.69 ± 4.51	248.81 ± 5.75^{a}	67.79 ± 3.75^{a}	$244.57 \pm 2.13^{a,b}$
14,15-EET	142.54 ± 5.32	360.52 ± 6.55^{a}	127.50 ± 4.73^{a}	$344.88 \pm 2.10^{a,b}$
5,6-DHET	0.78 ± 0.07	1.41 ± 0.08^{a}	0.53 ± 0.03^{a}	$1.17 \pm 0.08^{a,b}$
8,9-DHET	1.70 ± 0.06	6.01 ± 0.10^{a}	1.52 ± 0.05	$5.55 \pm 0.13^{a,b}$
11,12-DHET	2.65 ± 0.04	6.38 ± 0.18^{a}	2.55 ± 0.03	$5.95 \pm 0.23^{a,b}$
14,15-DHET	2.58 ± 0.16	6.99 ± 0.18^{a}	2.04 ± 0.10^{a}	$7.20 \pm 0.13^{a,b}$
LA-CYP epoxygenase				
12,13-EpOME	80.03 ± 2.73	82.08 ± 3.28	76.76 ± 2.41	79.30 ± 3.51
9,10-EpOME	98.24 ± 2.07	95.00 ± 3.43	102.42 ± 2.55	96.12 ± 2.98
12,13-diHOME	46.81 ± 2.49	50.42 ± 2.84	51.22 ± 3.28	53.27 ± 2.46
9,10-diHOME	31.22 ± 2.25	36.26 ± 3.20	35.13 ± 3.04	34.65 ± 3.53
AA-CYP allylic-oxidase				
9-HETE	148.75 ± 3.82	150.73 ± 3.56	187.66 ± 1.17^{a}	192.27 ± 1.91^{a}
11-HETE	105.75 ± 2.10	110.29 ± 2.10	143.18 ± 3.78^{a}	148.46 ± 5.02^{a}
AA-LOX				
15-HETE	154.15 ± 1.20	155.96 ± 1.24	197.26 ± 1.87^{a}	201.49 ± 2.24^{a}
5-HETE	188.28 ± 1.22	190.48 ± 1.04	237.41 ± 2.71^{a}	242.65 ± 2.65^{a}
8-HETE	64.10 ± 1.51	65.20 ± 1.14	85.08 ± 1.55^{a}	84.23 ± 1.32^{a}
AA-CYP ω-hydrolase				
16-HETE	4.55 ± 0.12	4.77 ± 0.13	4.95 ± 0.10	5.00 ± 0.22
17-HETE	1.48 ± 0.07	1.39 ± 0.08	1.59 ± 0.07	1.22 ± 0.05
18-HETE	1.56 ± 0.08	1.78 ± 0.09	1.70 ± 0.10	1.68 ± 0.09
19-HETE	1.77 ± 0.05	1.93 ± 0.13	2.01 ± 0.06	1.82 ± 0.03
20-HETE	0.48 ± 0.05	0.61 ± 0.06	1.63 ± 0.05^{a}	1.53 ± 0.03^{a}

Eicosanoid levels are in picograms per milligram. LC/MS/MS results revealed that EETs and DHETs in cardiac tissue were increased in αMHC-CYP2J2-Tr mice under both saline- and Ang II-infused condition (n = 5 for each group). LA, linoleic acid; EpOME, epoxy-12Z-octadecenoic acid; diHOME, dihydroxyoctadecenoic acid.
[a]$P < 0.05$ versus WT-saline.
[b]$P < 0.05$ versus WT-Ang II.

to EETs and did not influence levels of eicosanoids in other metabolic pathways, suggesting that the anti-fibrotic effects of CYP2J2 are specific for EETs.

CYP2J2 overexpression with elevation of EETs attenuates cardiac dysfunction and fibrosis

Echocardiography and hemodynamic assessments showed that CYP2J2 overexpression in heart attenuated Ang II-induced cardiac dysfunction (**Table 4**). Picrosirius red staining showed that Ang II induced markedly enhanced collagen accumulation in heart; however, these effects were attenuated in aMHC-CYP2J2-Tr mice (**Fig. 1A**, B). Similarly, the α-SMA- or COL I-positive area of aMHC-CYP2J2-Tr mice infused with Ang II was significantly decreased compared with controls (Fig. 1A, C, D).

Western blots were performed to examine expression of COL I, α-SMA, proliferation marker PCNA, and fibrosis-related transcription factor, myocardin-related transcription factor A (MRTF-A). CYP2J2 was expressed in CYP2J2 transgenic mice, but not in WT mice (Fig. 1E). CYP2J2 overexpression downregulated Ang II-induced expression of COL I and α-SMA in cardiac tissue (Fig. 1E, F). Moreover, PCNA and MRTF-A nuclear translocation induced by Ang II infusion were alleviated by CYP2J2 overexpression (Fig. 1G, H). However, sEH upregulation induced by Ang II was not inhibited by CYP2J2 overexpression (supplemental Fig. 4A).

Collectively, these results suggest that Ang II induces cardiac dysfunction and cardiac fibrosis, including enhanced collagen accumulation and increased myofibroblast transformation; these detrimental effects were associated with increased nuclear translocation of MRTF-A and PCNA. However, CYP2J2 overexpression attenuated these harmful effects induced by Ang II.

Inhibition of $G\alpha_{12/13}$/RhoA/ROCK signaling is involved in anti-fibrotic effects of CYP2J2 in cardiac tissue

As the $G_{\alpha12/13}$/RhoA/ROCK pathway is essential for Ang II-induced cardiac fibrosis and is a target of fibrotic disease, we, therefore, investigated the effects of CYP2J2 on this pathway. A GST pull down assay showed that CYP2J2 overexpression inhibited the elevation in activities of both $G\alpha_{12/13}$ and RhoA in cardiac tissue induced by Ang II (**Fig. 2A**–D). Moreover, the p-myosin phosphatase target subunit-1 (MYPT)/MYPT ratio, which reflects activity of ROCK, was reduced by CYP2J2 overexpression (Fig. 2E, F). Above all, CYP2J2 overexpression with elevation of EETs inhibited the $G\alpha_{12/13}$ activity and subsequent RhoA/ROCK activation in cardiac tissue. These results revealed that inhibition of $G\alpha_{12/13}$ activity and subsequent RhoA/ROCK activation are correlated with the anti-fibrotic effect of CYP2J2/EETs.

Fibrotic response of cardiac fibroblasts induced by Ang II is inhibited by 11,12-EET incubation

The fibroblasts isolated from neonatal rat heart were cultured and treated with Ang II to induce fibrotic response and, moreover, an exogenous EET role was observed. The

TABLE 2. Eicosanoids levels in plasma measured by LC/MS/MS

	Saline		Ang II	
	WT	αMHC-CYP2J2-Tr	WT	αMHC-CYP2J2-Tr
AA-CYP epoxygenase				
5,6-EET	15.49 ± 0.82	36.40 ± 2.34^a	8.92 ± 0.54^a	$30.53 \pm 3.23^{a,b}$
8,9-EET	14.42 ± 0.86	26.31 ± 1.28^a	9.84 ± 0.24^a	$22.14 \pm 2.02^{a,b}$
11,12-EET	18.39 ± 0.66	51.85 ± 1.34^a	13.90 ± 0.97^a	$44.97 \pm 2.26^{a,b}$
14,15-EET	22.97 ± 1.65	70.08 ± 1.68^a	17.55 ± 1.10^a	$61.09 \pm 2.19^{a,b}$
5,6-DHET	0.04 ± 0.01	0.79 ± 0.05^a	0.03 ± 0.01	$0.63 \pm 0.06^{a,b}$
8,9-DHET	0.70 ± 0.06	1.56 ± 0.10^a	0.66 ± 0.03	$1.37 \pm 0.09^{a,b}$
11,12-DHET	0.65 ± 0.04	6.37 ± 0.18^a	0.55 ± 0.03	$5.94 \pm 0.23^{a,b}$
14,15-DHET	1.21 ± 0.07	3.48 ± 0.14^a	1.12 ± 0.08	$3.10 \pm 0.08^{a,b}$
LA-CYP epoxygenase				
12,13-EpOME	22.00 ± 0.99	19.62 ± 1.28	20.94 ± 1.09	19.48 ± 1.43
9,10-EpOME	19.75 ± 1.80	18.66 ± 1.44	21.76 ± 1.73	20.56 ± 1.50
12,13-diHOME	49.90 ± 1.71	46.98 ± 2.29	48.67 ± 3.38	45.99 ± 2.34
9,10-diHOME	14.62 ± 1.30	15.96 ± 1.07	12.34 ± 0.88	13.97 ± 1.24
AA-CYP allylic-oxidase				
9-HETE	53.35 ± 1.23	55.91 ± 1.49	72.46 ± 2.09^a	70.70 ± 3.56^a
11-HETE	3.76 ± 0.17	3.48 ± 0.10	5.75 ± 0.12^a	5.90 ± 0.23^a
AA-LOX				
15-HETE	8.58 ± 0.13	9.14 ± 0.24	13.39 ± 0.23^a	13.95 ± 0.19^a
5-HETE	5.96 ± 0.17	5.55 ± 0.14	11.13 ± 0.31^a	10.94 ± 0.37^a
8-HETE	8.80 ± 0.32	9.14 ± 0.26	12.98 ± 0.44^a	13.56 ± 0.18^a
AA-CYP ω-hydrolase				
16-HETE	0.68 ± 0.08	0.70 ± 0.07	0.81 ± 0.06	0.63 ± 0.08
17-HETE	0.40 ± 0.03	0.46 ± 0.02	0.43 ± 0.02	0.36 ± 0.03
18-HETE	0.75 ± 0.10	0.71 ± 0.07	0.73 ± 0.08	0.69 ± 0.06
19-HETE	0.35 ± 0.05	0.33 ± 0.04	0.40 ± 0.03	0.30 ± 0.04
20-HETE	0.30 ± 0.02	0.32 ± 0.02	1.54 ± 0.12^a	1.43 ± 0.09^a

Eicosanoids levels are in nanograms per milliliter. LC/MS/MS results revealed that EETs and DHETs in plasma were increased in αMHC-CYP2J2-Tr mice under both saline- and Ang II-infused condition (n = 5 for each group). LA, linoleic acid; EpOME, epoxy-12Z-octadecenoic acid; diHOME, dihydroxyoctadecenoic acid.
$^a P < 0.05$ versus WT-saline.
$^b P < 0.05$ versus WT-Ang II.

11,12-EET was most effective in inhibiting upregulation of COL I and α-SMA induced by Ang II (supplemental Fig. S1A). Moreover, effects of 11,12-EET on α-SMA were dose-dependent (supplemental Fig. S1B). Based on these results, 11,12-EET, at a concentration of 1 μM, was used for the following experiments. Immunofluorescence staining showed that 11,12-EET reduced the numbers of α-SMA and nuclear PCNA immunofluorescence-positive cells induced by Ang II, revealing that 11,12-EET alleviates myofibroblast transformation and proliferation (**Fig. 3A–C**). A transwell assay was performed to determine the migration ability of cardiac fibroblasts and results showed that 11,12-EET attenuated Ang II-induced fibroblast migration (Fig. 3D, E). Consistent with in vivo findings, 11,12-EET reduced expression of COL I and α-SMA induced by Ang II (Fig. 3F, G). Moreover, nuclear translocation of PCNA and MRTF-A induced by Ang II were inhibited by 11,12-EET (Fig. 3H, I). However, all the anti-fibrotic effects of 11,12-EET were blocked by putative EET receptor antagonist, 14,15-EEZE (Fig. 3). These results suggest that 11,12-EET inhibits cardiac fibrotic response, including cardiac fibroblast transformation, proliferation, migration, and collagen secretion.

Gα$_{12/13}$/RhoA/ROCK cascade inhibition is involved in anti-fibrotic effects of 11,12-EET in cardiac fibroblasts

The well-established downstream effectors of Gα$_{12/13}$-mediated signaling are the monomeric GTPase, RhoA, and the RhoA effector, ROCK, which are regulators of a variety of intracellular processes, including actin stress fiber formation, cell movement, and growth. In an in vivo study, we have demonstrated that inhibition of the Gα$_{12/13}$/RhoA/ROCK pathway was involved in anti-fibrotic effects of CYP2J2. To further identify whether inhibition of the Gα$_{12/13}$/RhoA/ROCK pathway was involved in anti-fibrotic effects of EETs in cardiac fibroblasts, we detected Gα$_{12/13}$/RhoA/ROCK pathway activation in cardiac fibroblasts under various treatments. First, we detected activation of Gα$_{12/13}$ and RhoA induced by Ang II under different concentrations and various time points. Results showed that Ang II at a concentration of 1 μM was the most powerful to induce activation of Gα$_{12/13}$ and RhoA and the effects remained from 5 to 10 min (supplemental Fig. 2A–D). Therefore, the Ang II (1 μM) for 5 min treatment was used for inducing activation of Gα$_{12/13}$ and RhoA in the following experiment. Moreover, 11,12-EET inhibited activation of Gα$_{12/13}$ and RhoA induced by Ang II in cardiac fibroblasts (**Fig. 4A–C**) and these effects remained from 5 to 10 min (supplemental Fig. S2E, F). Furthermore, the p-MYPT/MYPT ratio, which reflects activity of ROCK, was reduced by 11,12-EET as well (Fig. 4D). The anti-fibrotic effects of 11,12-EET were blocked by the putative EET receptor antagonist, 14,15-EEZE (Fig. 4). We also detected PLCβ phosphorylation, the main effector pathway of G$_{q/11}$, could not be affected by 11,12-EET (supplemental Fig. S4B). Above all, these results indicated that inhibition of Gα$_{12/13}$/RhoA/ROCK activities is involved in the anti-fibrotic effects of 11,12-EET.

TABLE 3. Eicosanoids levels in cultured medium measured by LC/MS/MS

	Saline		Ang II	
	WT	αMHC-CYP2J2-Tr	WT	αMHC-CYP2J2-Tr
AA-CYP epoxygenase				
5,6-EET	17.8 ± 0.86	85.81 ± 4.72^{a}	7.00 ± 0.55^{a}	$84.80 \pm 4.97^{a,b}$
8,9-EET	30.42 ± 2.00	126.22 ± 1.23^{a}	24.840 ± 1.66^{a}	$119.25 \pm 2.16^{a,b}$
11,12-EET	60.00 ± 2.36	314.00 ± 10.30^{a}	33.40 ± 1.89^{a}	$312.00 \pm 13.93^{a,b}$
14,15-EET	56.00 ± 2.91	148.00 ± 5.83^{a}	34.00 ± 2.92^{a}	$140.00 \pm 4.47^{a,b}$
5,6-DHET	12.00 ± 0.34	42.05 ± 0.68^{a}	11.36 ± 0.46	$40.44 \pm 0.60^{a,b}$
8,9-DHET	14.39 ± 0.49	47.03 ± 0.67^{a}	12.84 ± 0.59	$43.35 \pm 1.15^{a,b}$
11,12-DHET	27.55 ± 1.26	88.24 ± 1.59^{a}	23.87 ± 0.73	$84.65 \pm 1.19^{a,b}$
14,15-DHET	70.62 ± 1.73	171.67 ± 4.09^{a}	67.56 ± 1.65	$161.07 \pm 3.32^{a,b}$
LA-CYP epoxygenase				
12,13-EpOME	46.09 ± 2.00	47.77 ± 2.29	43.85 ± 2.29	45.50 ± 2.15
9,10-EpOME	67.71 ± 2.95	72.04 ± 2.50	70.33 ± 3.00	69.00 ± 1.91
12,13-diHOME	70.61 ± 1.62	73.30 ± 2.52	69.45 ± 2.12	68.86 ± 3.41
9,10-diHOME	58.84 ± 2.41	57.62 ± 2.56	55.50 ± 1.29	56.37 ± 2.24
AA-CYP allylic-oxidase				
9-HETE	46.15 ± 1.63	45.87 ± 1.34	75.57 ± 1.86^{a}	75.93 ± 1.88^{a}
11-HETE	111.30 ± 3.62	108.44 ± 2.81	150.35 ± 2.38^{a}	147.86 ± 2.85^{a}
AA-LOX				
15-HETE	107.93 ± 2.20	105.94 ± 1.87	147.89 ± 1.97^{a}	150.70 ± 3.12^{a}
5-HETE	26.61 ± 1.26	22.53 ± 0.95	40.04 ± 2.46^{a}	39.77 ± 3.59^{a}
8-HETE	69.05 ± 2.65	73.64 ± 2.37	110.24 ± 2.67^{a}	108.77 ± 2.58^{a}
AA-CYP ω-hydrolase				
16-HETE	6.39 ± 0.17	7.08 ± 0.28	6.83 ± 0.26	6.73 ± 0.30
17-HETE	3.52 ± 0.10	3.71 ± 0.85	3.86 ± 0.10	4.04 ± 0.86
18-HETE	14.96 ± 0.41	15.05 ± 0.43	16.16 ± 0.50	15.67 ± 0.61
19-HETE	14.09 ± 0.31	13.77 ± 0.28	14.24 ± 0.23	13.91 ± 0.28
20-HETE	13.72 ± 0.46	13.12 ± 0.19	22.81 ± 0.22^{a}	23.49 ± 0.52^{a}

Eicosanoids levels are in picograms per milliliter. LC/MS/MS results revealed that secretion of EETs and DHETs were increased in cardiomyocytes from αMHC-CYP2J2-Tr mice under both saline- and Ang II-infused condition (n = 5 for each experiment). LA, linoleic acid; EpOME, epoxy-12Z-octadecenoic acid; diHOME, dihydroxyoctadecenoic acid.
[a]$P < 0.05$ versus WT-saline.
[b]$P < 0.05$ versus WT-Ang II.

The 11,12-EET attenuated Ang II-induced fibrotic response of cardiac fibroblasts by inhibiting the Gα$_{12/13}$/RhoA /ROCK signaling pathway

To further elucidate whether 11,12-EET attenuated Ang II-induced fibrotic response via the Gα$_{12/13}$/RhoA/ROCK signaling pathway, siRNA was used to knock down Gα$_{12/13}$ or RhoA. Western blots showed that Gα$_{12/13}$ or RhoA knockdown by their corresponding siRNAs, as well as incubation of 11,12-EET, attenuated activity of the RhoA effector, ROCK (**Fig. 5J**). Results of immunofluorescence staining showed that silencing of Gα$_{12/13}$ or RhoA, as well as 11,12-EET, reduced the numbers of α-SMA or nuclear PCNA immunofluorescence-positive cells induced by Ang II (Fig. 5A, C, D), which indicates that silencing Gα$_{12/13}$ or RhoA, as well as 11,12-EET, alleviates myofibroblast transformation and proliferation. A transwell assay was performed to determine the migration ability of cardiac fibroblasts and the results revealed that specific knockdown of Gα$_{12/13}$ or RhoA by siRNA or 11,12-EET attenuated Ang II-induced migration of fibroblasts (Fig. 5B, E).

TABLE 4. Hemodynamic and echocardiography results

	Saline		AngII	
	WT	αMHC-CYP2J2-Tr	WT	αMHC-CYP2J2-Tr
Hemodynamic				
HR (bmp)	424 ± 6	425 ± 5	431 ± 5	427 ± 5
LVEDP (mmHg)	4.23 ± 0.04	4.19 ± 0.04	7.73 ± 0.09^{a}	5.42 ± 0.08^{b}
dp/dt max (mmHg/s)	$5,998 \pm 20$	$6,020 \pm 18$	$2,793 \pm 17^{a}$	$4,107 \pm 17^{b}$
dp/dt min (mmHg/s)	$4,632 \pm 17$	$4,593 \pm 24$	$1,817 \pm 23^{a}$	$3,106 \pm 21^{b}$
Echocardiography				
Ejection fraction (%)	81 ± 0.3	80 ± 0.3	47 ± 0.4^{a}	70 ± 0.3^{b}
Fraction shortening (%)	39.7 ± 0.4	39.6 ± 0.4	26.5 ± 0.3^{a}	37.4 ± 0.3^{b}
LVID (d) (mm)	3.57 ± 0.04	3.58 ± 0.04	4.63 ± 0.03^{a}	3.77 ± 0.02^{b}
LVID (s) (mm)	2.60 ± 0.03	2.54 ± 0.04	3.39 ± 0.03^{a}	2.94 ± 0.04^{b}

dp/dt max, maximal slope of systolic pressure increment; dp/dt min, minimal slope of diastolic pressure decrement; LVID (d), left ventricular internal dimension in diastole; LVID (s), left ventricular internal dimension in systole; LVEDP, left ventricular end diastolic pressure; HR, heart rate; CYP2J2, CYP2J2 transgenic mice (n = 10 for each group).
[a]$P < 0.05$ versus WT-saline.
[b]$P < 0.05$ versus WT-Ang II.
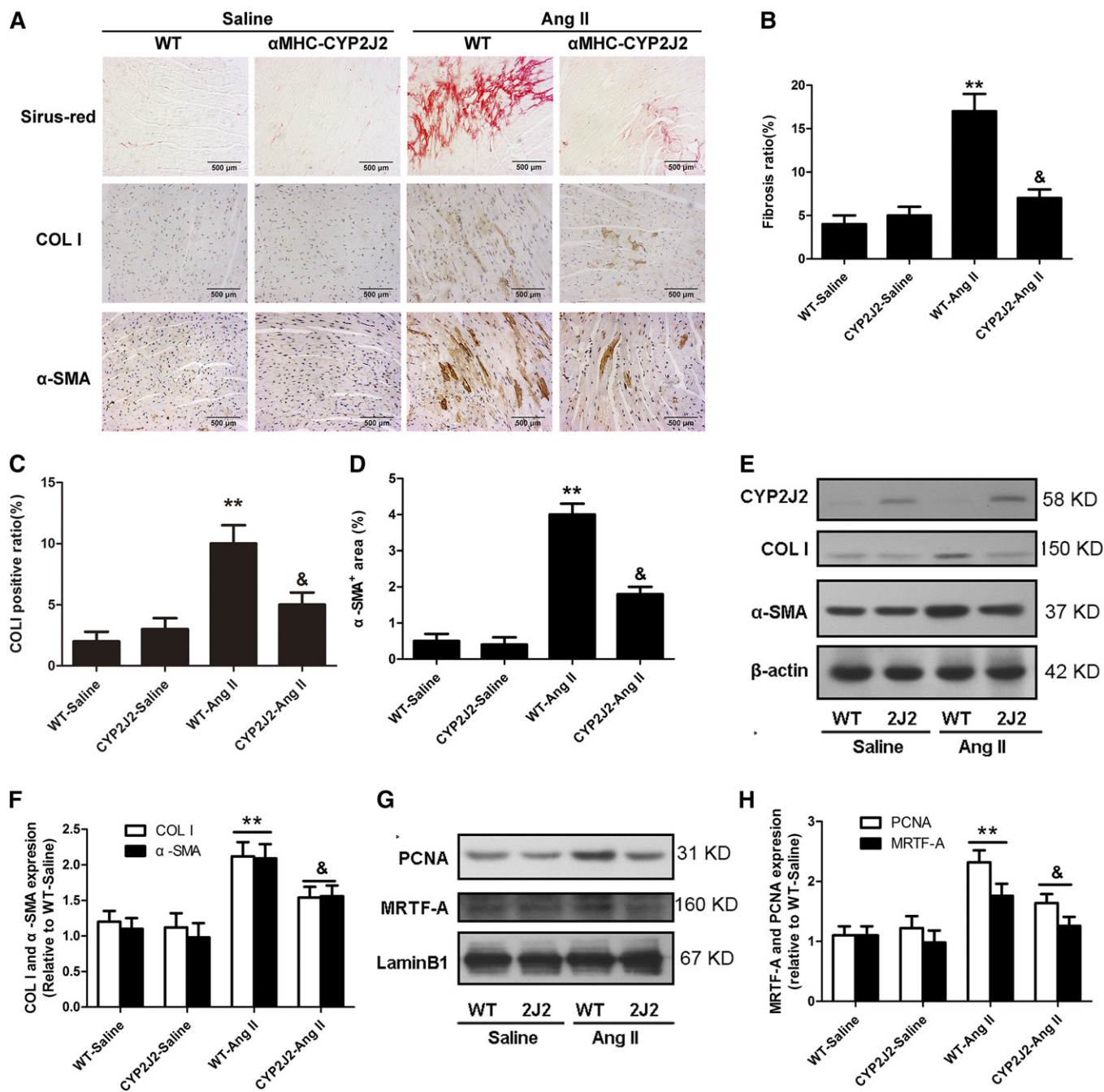
Fig. 1. Expression of CYP2J2 in cardiomyocytes prevents the development of Ang II-induced cardiac fibrosis. A: Evaluation of collagen deposition by picrosirius red staining, histological analysis of cardiac fibroblast transformation and collagen secretion by immunohistochemical staining of α-SMA and COL I, respectively. B: Quantitation of cardiac fibrosis. C: Quantitation of COLI-positive area. D: Quantitation of α-SMA-positive area. E: Representative immunoblots for CYP2J2, COL I, and α-SMA. F: Quantitation of COL I and α-SMA expression in cardiac tissue. G: Representative immunoblots for nuclear PCNA and MRTF-A in cardiac tissue. H: Quantitation of nuclear PCNA and MRTF-A in cardiac tissue. $**P < 0.05$ versus WT-saline; $^{\&}P < 0.05$ versus WT-Ang II (n = 10 for each group).

In line with the morphological results, COL I and α-SMA, as well as the nuclear translocation of MRTF-A and PCNA, were attenuated by specific knockdown of $G\alpha_{12/13}$ or RhoA by siRNA or 11,12-EET (Fig. 5F–I). Above all, reduced expression of $G\alpha_{12/13}$ or RhoA exerts similar effects as 11,12-EET on inhibition of fibrotic response. These results suggest that EETs alleviate cardiac fibrotic response by inhibiting the $G\alpha_{12/13}$/RhoA/ROCK pathway.

The 11,12-EET attenuates $G\alpha_{12/13}$ activity via activating the NO/cGMP pathway

Next, we detected the content of NO/cGMP in cardiac tissue and cultured cardiac fibroblasts. Results showed that CYP2J2 overexpression elevated NO and cGMP levels in cardiac tissue and similar effects were observed in cardiac fibroblasts with 11,12-EET treatment (**Fig. 6A**, B). Moreover, 11,12-EET attenuated Ang II-induced $G\alpha_{12/13}$ activation. However, the inhibition of $G\alpha_{12/13}$ by 11,12-EET was
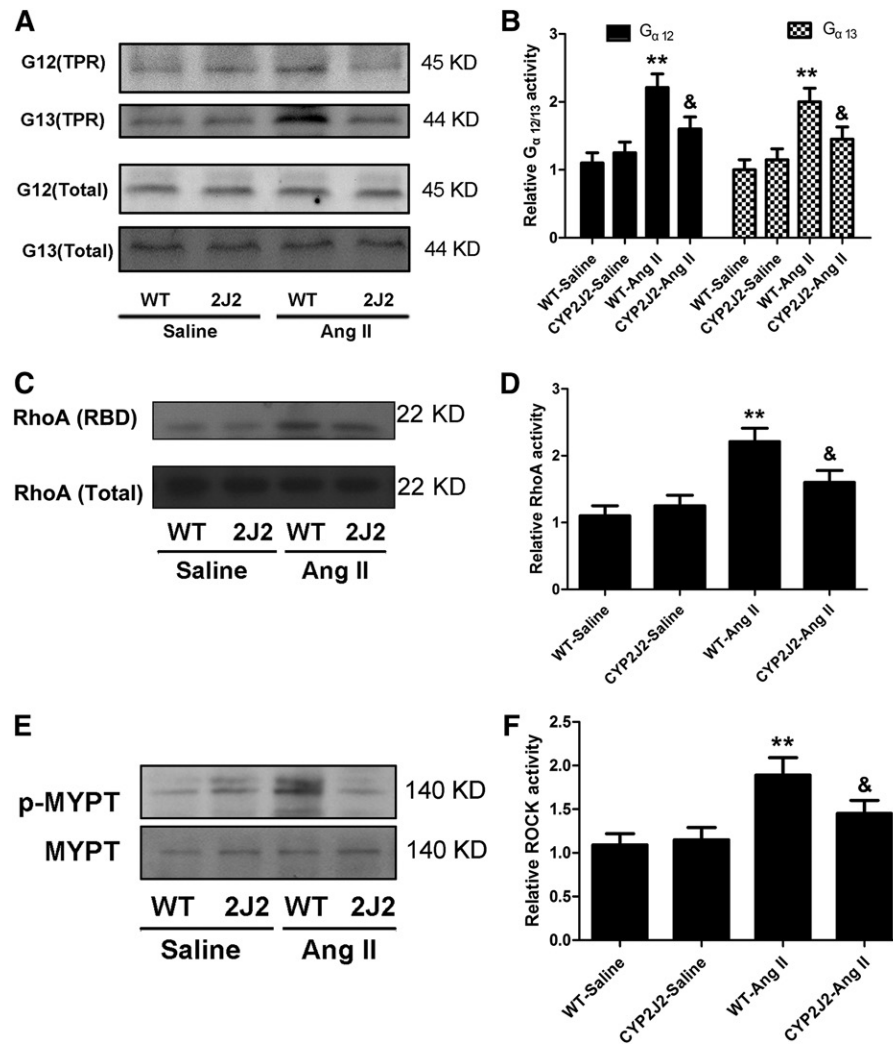
Fig. 2. Inhibition of the $G\alpha_{12/13}$/RhoA/ROCK pathway is involved in the anti-fibrotic effects of CYP2J2. A: Representative immunoblots of G12 (TPR), G12 (Total), G13 (TPR), and G13 (Total) in cardiac tissue. B: Quantitation of $G\alpha_{12}$ activity and $G\alpha_{13}$ activity by determining the ratio of G12 (TPR)/G12 (Total) and G13 (TPR)/G13 (Total), respectively. C: Representative immunoblot of RhoA (RBD) and RhoA in cardiac tissue. D: Quantitation of RhoA activity by the ratio between RhoA (RBD) and RhoA (Total). E: Representative immunoblot of p-MYPT and MYPT in cardiac tissue. F: ROCK activity was evaluated by the ratio between p-MYPT and MYPT. ** $P < 0.05$ versus WT-saline; & $P < 0.05$ versus WT-Ang II (n = 10 for each group).

partially blocked by selective eNOs inhibitor, L-N^5-(1-imi-noethyl)ornithine hydrochloride, NO scavenger, hydroxo-cobalamin, or guanylate cyclase inhibiter, 1H-[1,2,4] oxadiazolo[4,3-a]quinoxalin-1-one (Fig. 6C, D). These results suggest that CYP2J2 overexpression or 11,12-EET attenuates $G\alpha_{12/13}$ activity by activating the NO/cGMP pathway.

DISCUSSION

Main findings

The present work identified that CYP2J2 overexpression with elevation of EETs inhibited Ang II-induced cardiac dysfunction and cardiac fibrosis. Furthermore, we elucidated the underlying mechanisms: *1)* Cardiomyocyte-specific expression of CYP2J2 increases EET release from cardiomyocytes, which results in inhibition of the fibrotic response of cardiac fibroblasts, including cardiac fibroblast proliferation, transformation, migration, and collagen secretion. *2)* Our data provides new evidence that EETs inhibit fibrotic response of cardiac fibroblasts by targeting $G\alpha_{12/13}$ protein and subsequent RhoA/ROCK signaling activation. *3)* EETs inhibit Ang II-induced $G\alpha_{12/13}$ activation via NO/cGMP signaling.
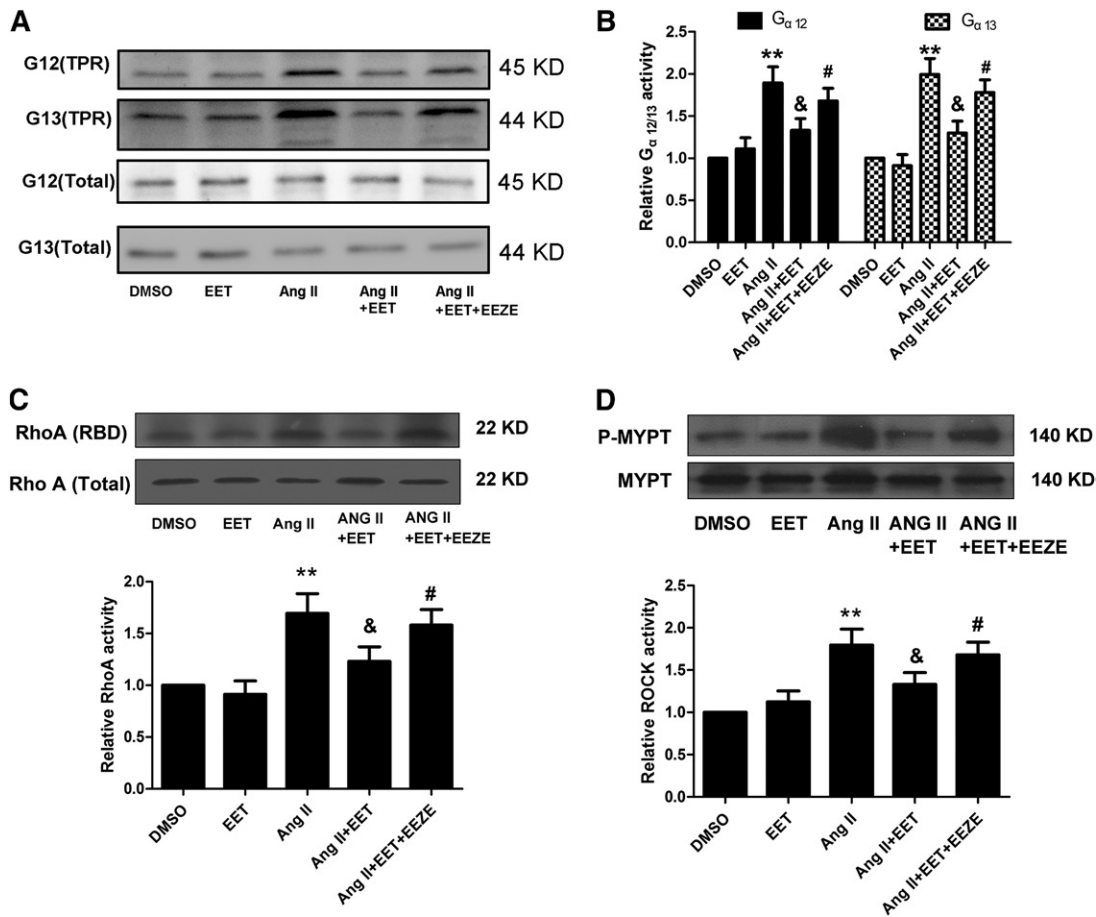
Direct effects of EETs on cardiac fibroblasts are an important mechanism that contributes to the protective effects of EETs

Cardiac hypertrophy and fibrosis is a complicated pathophysiological process and EETs have multiple biological functions, so our group did a series of works in this field. Our present and previous works have demonstrated that cardiac and systemic EET levels were increased in αMHC-CYP2J2-Tr mice (13). Moreover, EETs that are able
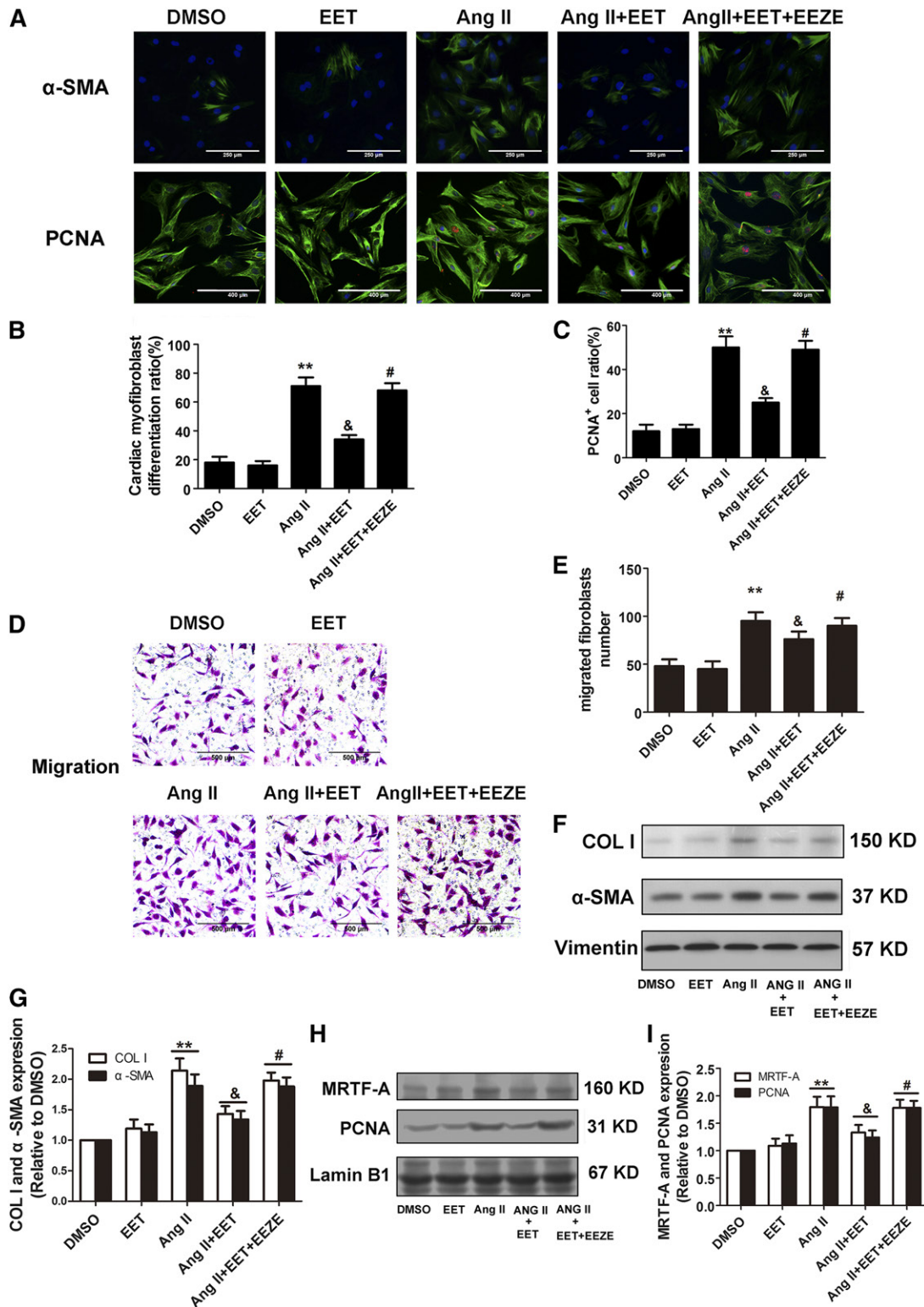
Fig. 3. Treatment of neonatal rat cardiac fibroblasts with 11,12-EET inhibits Ang II-induced fibrotic response in cardiac fibroblasts, including cardiac fibroblast transformation, proliferation, migration, and collagen secretion. A: Representative immunofluorescent images of α-SMA-positive cells and PCNA-positive cells in cultured neonatal rat cardiac fibroblasts treated with various reagents for 24 h. B: Quantitation of α-SMA-positive cells in (A). C: Quantitation of PCNA-positive cells in (A). D: Representative images of migrated fibroblasts treated with various reagents for 6 h. E: Quantitation of migrated fibroblasts in (D). F: Representative immunoblots for COL I and α-SMA in cultured neonatal rat cardiac fibroblasts treated with various reagents for 24 h. G: Quantitation of COL I and α-SMA in cardiac fibroblasts. H: Representative immunoblots for nuclear PCNA and MRTF-A in cultured neonatal rat cardiac fibroblasts treated with various reagents for 24 h. I: Quantitation of nuclear PCNA and MRTF-A in cardiac fibroblasts. $**P < 0.05$ versus DMSO; $^{\&}P < 0.05$ versus Ang II; $^{\#}P < 0.05$ versus Ang II + 11,12-EET (n = 5 for each experiment).

Fig. 4. Inhibition of the $G\alpha_{12/13}$/RhoA/ROCK pathway is involved in the anti-fibrotic effects of EETs. A: Representative immunoblots of G12 (TPR), G12 (Total), G13 (TPR), and G13 (Total) in cardiac fibroblasts treated with various reagents for 5 min. B: Quantitation of $G\alpha_{12}$ activity and $G\alpha_{13}$ activity by determining the ratio of G12 (TPR)/G12 (Total) and G13 (TPR)/G13 (Total), respectively. C: Representative immunoblot of RhoA (RBD) and RhoA (Total) and quantitation of RhoA activity by the ratio between RhoA (RBD) and RhoA (Total) in cardiac fibroblasts treated with various reagents for 5 min. D: Representative immunoblot of p-MYPT and MYPT and quantitation of ROCK activity by the ratio between p-MYPT and MYPT in cardiac fibroblasts treated with various reagents for 5 min. **$P < 0.05$ versus DMSO; &$P < 0.05$ versus Ang II; #$P < 0.05$ versus Ang II + 11,12-EET (n = 5 for each experiment).

to release into the extracellular fluid can produce paracrine and autocrine effects in the local environment (43), so EETs could act on cardiomyocytes, cardiac fibroblasts, and immune cells. In previous research, the cardio-protective effects of CYP2J2/EETs by acting directly on cardiomyocytes were elucidated. EETs can suppress cardiac dysfunction and remodeling through inhibiting the elevation of the intracellular Ca^{2+} level and subsequent ER stress response via upregulating and stabilizing SERCA2a by anti-oxidative stress (8). However, this previous work did not illustrate the anti-oxidative stress mechanism of EETs. Furthermore, other research was performed illustrating that EETs could inhibit oxidative stress by activating PPAR-γ (13). Interestingly, we have found that CYP2J2 and EETs enhanced Akt1 nuclear translocation through interaction with AMPKα2β2γ1 and protected against cardiac hypertrophy (14). As cellular cross-talk contributes largely to cardiac remodeling, we studied the effects and mechanisms of EETs on cross-talk between cardiomyocytes, cardiac fibroblasts, and macrophages. We have found that EETs inhibited cardiac fibrosis by alleviating pro-fibrotic and pro-inflammatory responses

of cardiomyocytes that were transmitted to cardiac fibroblasts and macrophages, respectively (13, 15). Cardiac fibroblasts constitute two-thirds of all cells in the heart and are the main source of extracellular matrix (2, 44). However, the direct effects of EETs on cardiac fibroblasts have not been elucidated. In the present studies, we identified that CYP2J2 overexpression with elevation of EETs inhibited Ang II-induced cardiac dysfunction and cardiac fibrosis by directly acting on cardiac fibroblasts, including inhibition of cardiac fibroblast transformation, proliferation, migration, and collagen secretion. The anti-fibrotic effects of 11,12-EET were blocked by the putative EET antagonist, 14,15-EEZE. DHETs, the stable and less bioactive diols of EETs, were elevated by CYP2J2 expression; however, they could not affect fibrotic response in cardiac fibroblasts, suggesting that the anti-fibrotic effects are abolished after sEH-mediated hydrolysis to the corresponding DHETs. This result was also supported by previous studies that showed that conversion of EETs to DHETs by sEH enzyme is responsible for decreasing EET levels and, thus, diminishing their beneficial cardiovascular properties (45, 46). Levels of eicosanoids in other
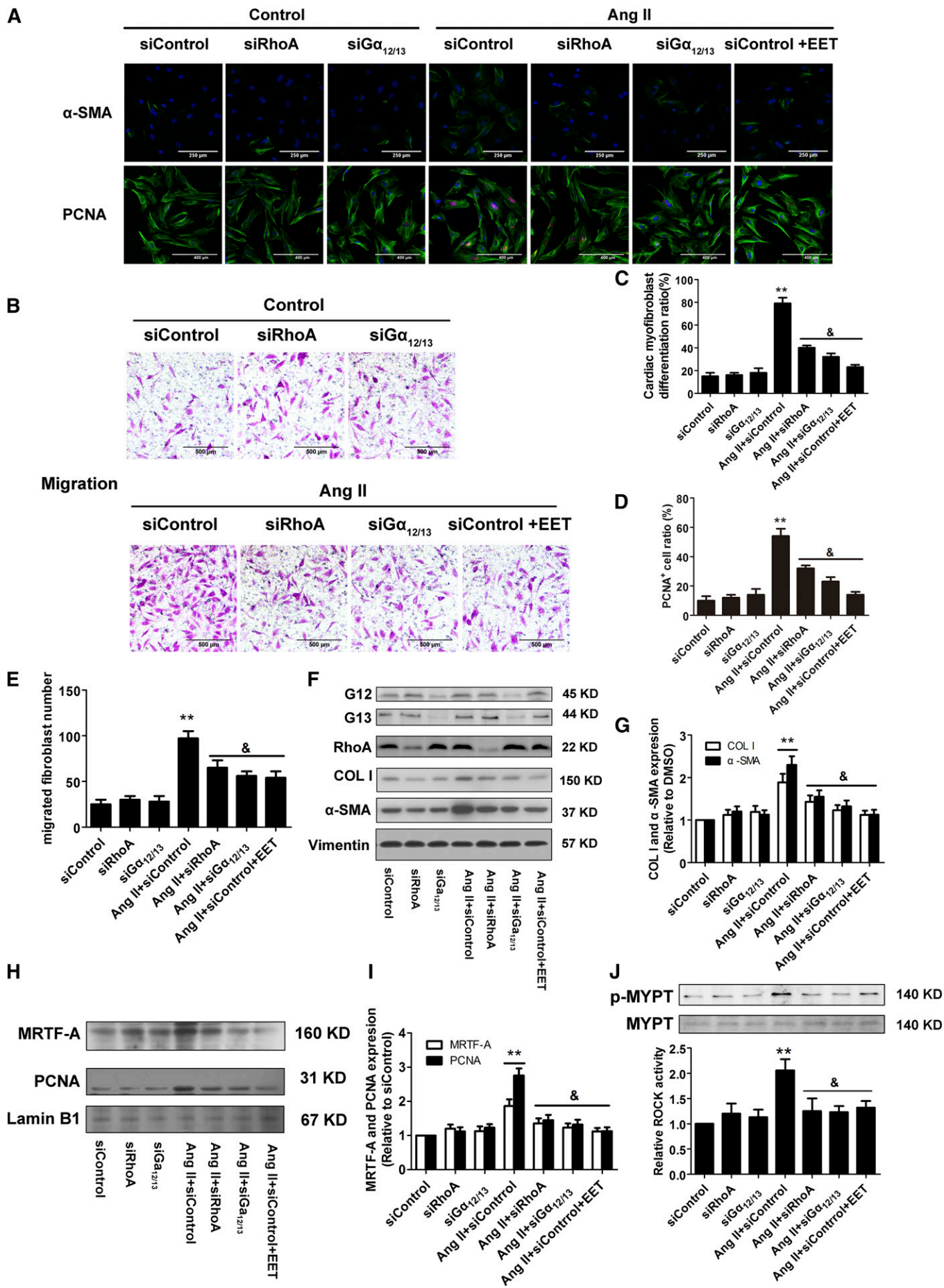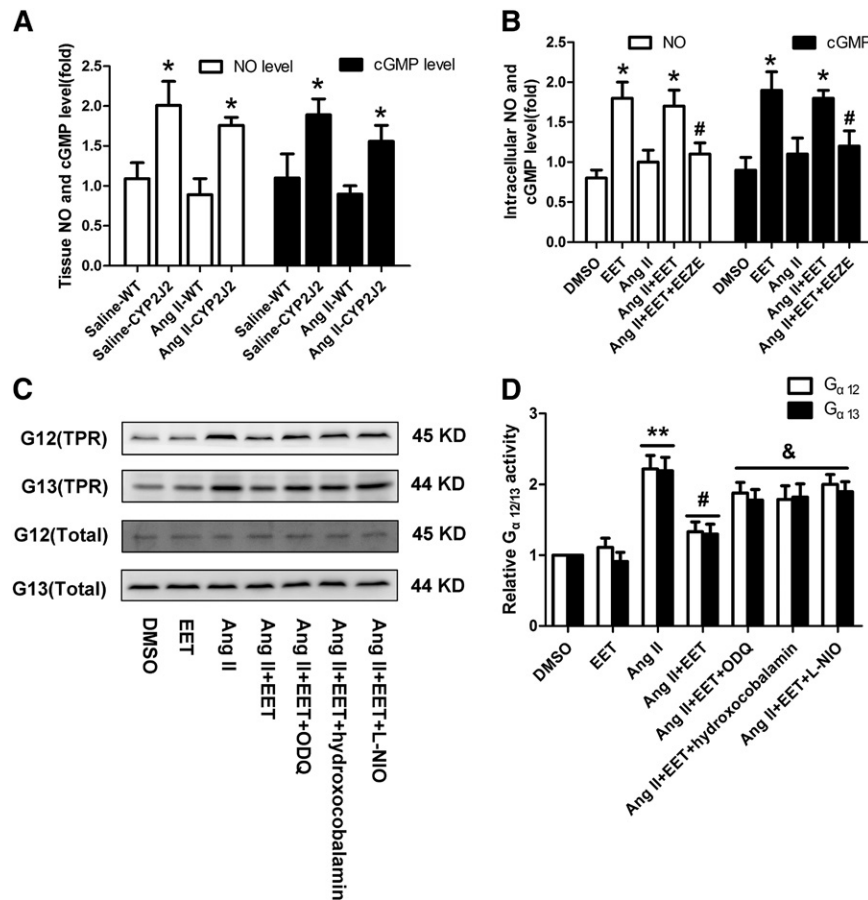
Fig. 6. Cardiomyocyte specific expression of CYP2J2 or treatment with 11,12-EET attenuate Ang II-induced G$\alpha_{12/13}$ activity via NO/cGMP activation. A: Quantitation of NO and cGMP level in cardiac tissue. NO concentration (picomoles per milligram protein): Saline-WT, 2.725 ± 0.50; Saline-Ang II, 5.025 ± 0.75; Ang II-WT, 2.225 ± 0.50; Ang II-CYP2J2, 4.400 ± 0.25. cGMP concentration (picomoles per milligram protein): Saline-WT, 0.1650 ± 0.045; Saline-CYP2J2, 0.2835 ± 0.030; Ang II-WT, 0.1350 ± 0.015; Ang II-CYP2J2, 0.2340 ± 0.030. *$P <$ 0.05 versus WT-saline (n = 5 for each group). B: Quantitation of NO and cGMP level in cardiac fibroblasts treated with various reagents for 5 min. NO concentration (picomoles per milligram protein): DMSO, 1.68 ± 0.210; EET, 3.78 ± 0.420; Ang II, 2.10 ± 0.315; Ang II + EET, 3.57 ± 0.420; Ang II + EET + EEZE, 2.31 ± 0.294. cGMP concentration (picomoles per milligram protein): DMSO, 0.117 ± 0.0208; EET, 0.246 ± 0.0299; Ang II, 0.143 ± 0.0260; Ang II + EET, 0.234 ± 0.0130; Ang II + EET + EEZE, 0.156 ± 0.0247. *$P <$ 0.05 versus DMSO; [#]$P <$ 0.05 versus Ang-II + 11,12-EET (n = 5 for each experiment). C: Representative immunoblots of G12 (TPR), G12 (Total), G13 (TPR), and G13 (Total) in cardiac fibroblasts treated with various reagents for 5 min. D: Quantitation of Gα_{12} activity and Gα_{13} activity by determining the ratio of G12 (TPR)/G12 (Total) and G13 (TPR)/G13 (Total), respectively. **$P <$ 0.05 versus DMSO; [#]$P <$ 0.05 versus Ang II; [&]$P <$ 0.05 versus Ang II + 11,12-EET (n = 5 for each experiment).

metabolic pathways were not influenced in transgenic mice in vivo and in vitro. Moreover, 17,18-EEQ, the predominant EPA epoxide, could not inhibit Ang II-induced upregulation of COL I and α-SMA. These results suggest that the anti-fibrotic effects of CYP2J2 are specifically mediated by EETs. The present work is a new and important component of our systematic and persistent research in the field of preventing cardiac hypertrophy and fibrosis. We have summarized previous and present works in a scheme picture (**Fig. 7**).

Fig. 5. siRNA mediated knockdown of G$\alpha_{12/13}$ or RhoA inhibits Ang II-induced fibrotic response in cardiac fibroblasts, including cardiac fibroblast transformation, proliferation, migration, and collagen secretion. A: Representative immunofluorescent images of α-SMA-positive cells and PCNA-positive cells in cultured neonatal rat cardiac fibroblasts treated with and without Ang II or various siRNAs for 24 h. B: Representative image of migrated fibroblasts treated with and without Ang II or various siRNAs for 6 h. C: Quantitation of α-SMA-positive cells. D: Quantitation of PCNA-positive cells. E: Quantitation of migrated fibroblasts. F: Representative immunoblots for Gα_{12}, Gα_{13}, RhoA, COL I, and α-SMA in cardiac fibroblasts treated with and without Ang II or various siRNA for 24 h. G: Quantitation of COL I and α-SMA in cardiac fibroblasts. H: Representative immunoblots for nuclear PCNA and MRTF-A in cardiac fibroblasts treated with and without Ang II or various siRNAs for 24 h. I: Quantitation of nuclear PCNA and MRTF-A in cardiac fibroblasts. J: Representative immunoblot of p-MYPT and MYPT and quantitation of ROCK activity by the ratio between p-MYPT and MYPT in cardiac fibroblasts treated with and without Ang II or various siRNAs for 5 min. **$P <$ 0.05 versus siControl; [&]$P <$ 0.05 versus Ang II + siControl (n = 5 for each experiment).
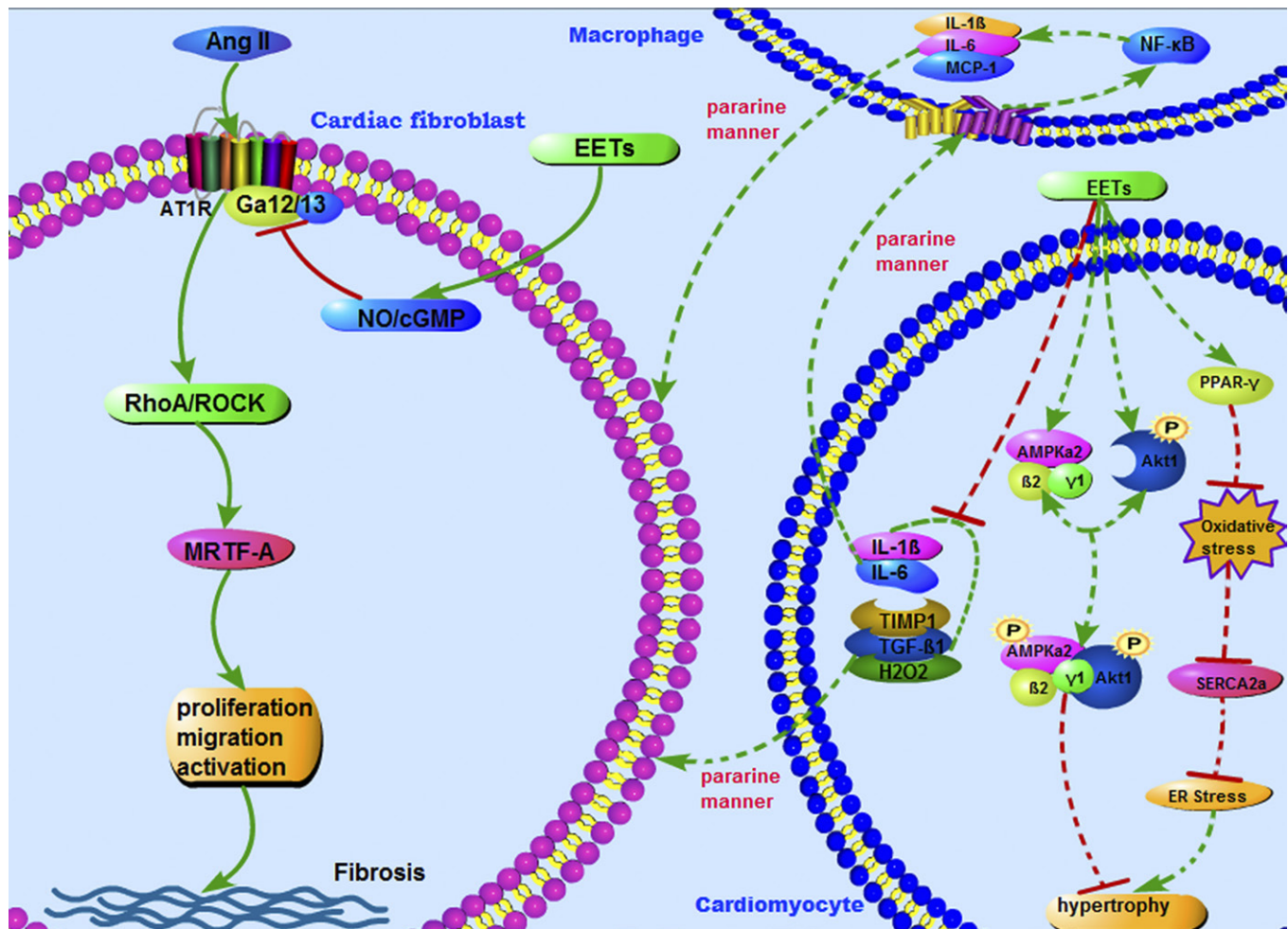
Fig. 7. Schematic of mechanisms on EET-mediated signaling in response to cardiac hypertrophy and fibrosis. EETs inhibit cardiac hypertrophy by acting directly on cardiomyocytes through the PPAR-γ/oxidative stress/SERCA2a/ER stress pathway and interaction of Akt1 and AMPKα2β2γ1 (8, 13, 14). Moreover, EETs attenuate pro-fibrotic and pro-inflammatory responses of cardiomyocytes transmitted to cardiac fibroblasts and macrophages, respectively (13, 15). This study indicates that EETs inhibit cardiac fibrosis by inhibiting fibrotic response of cardiac fibroblasts, including inhibition of cardiac fibroblast activation, proliferation, migration, and collagen secretion. Mechanistically, EETs stimulate the NO/cGMP signaling pathway, which reduces $G\alpha_{12/13}$ and subsequently inhibits RhoA/ROCK activation (Dashed lines represent previous findings and solid lines represent present findings).

The role of the NO/cGMP pathway for $G\alpha_{12/13}$ inhibition by EETs

The signal transduction induced by NO is performed intracellularly by its second messenger, cGMP, which exerts its effects via cGMP-dependent kinases, channels, or phosphodiesterases (47, 48). In this study, we found that CYP2J2 overexpression or EET treatment elevated the NO/cGMP level in cardiac tissue and cardiac fibroblasts, respectively. Moreover, inhibition of $G\alpha_{12/13}$ activity by EETs was blocked by NO/cGMP pathway inhibitors, suggesting that EETs attenuate $G\alpha_{12/13}$ activity via the NO/cGMP pathway. Some research supported this concept; previous research has demonstrated that EETs are able to stimulate eNOs activity and elevate NO level (26–28) and, moreover, that NO elevation by eNOS gene transfer or pharmacological treatment inhibits the $G\alpha_{12/13}$/RhoA/ROCK pathway (29, 49). How does the NO/cGMP pathway stimulated by EETs result in an inactivation of $G\alpha_{12/13}$? As previous studies have demonstrated that $G\alpha_{12}$ and $G\alpha_{13}$ possess a potential phosphorylation site for PKG (R/K-R/K-X-S/T) and, therefore, could be phosphorylated, the phosphorylation motif and surrounding sequences are well-conserved beyond the species in the subunits of $G\alpha_{12/13}$, but not in the subunits of other G proteins (29). We postulated that the inhibition effects of EETs on $G\alpha_{12/13}$ were attributed to $G\alpha_{12/13}$ phosphorylation by PKG because EETs were able to stimulate the NO/cGMP pathway (26, 50). This postulation was supported by previous studies where NO/cGMP/PKG cascade activation by eNOS gene-transfer or pharmacological treatment markedly enhanced $G\alpha_{13}$ phosphorylation in this conserved motif and subsequently inhibited RhoA activation in SMCs (29, 49). Furthermore, we postulated that PKG-mediated phosphorylation of $G\alpha_{12/13}$ might inhibit its interaction with $G_{\beta\gamma}$ leading to reduced $G\alpha_{12/13}$ activity, as a previous study has demonstrated that PKC phosphorylates $G\alpha_{12}$ and inhibits its interaction with $G_{\beta\gamma}$ (51). In the current study, we first provided evidence that $G\alpha_{12/13}$ was a new target of EETs and that NO/cGMP pathway activation mediated this process.

The role of $G\alpha_{12/13}$ activity inhibition in protective effects of CYP2J2/EET

Previous research has excluded the antagonism effects of EETs on the AT1R (16). Therefore, we sought to investigate whether the anti-fibrotic effects of 11,12-EET were mediated by antagonizing downstream mediators of AT1R. Ang II, a critical neurohumoral factor during myocardial damage, induces cardiac fibrosis through its receptor AT1R, which is coupled with G proteins, such as $G\alpha_{12/13}$, $G\alpha_{q/11}$, $G\alpha$s, $G\alpha$t, and $G\alpha_{i/o}$ (52). Previous studies have demonstrated that many GPCRs can influence Rho activities via signaling through both $G\alpha_{q/11}$ and $G\alpha_{12/13}$ families of heterotrimeric G proteins. $G\alpha_{12/13}$-mediated RhoA activation involves direct interactions with RhoGEF proteins, e.g., PDZ-RhoGEF, LARG, and p115-RhoGEF (53), and subsequent activation of pro-fibrotic signaling (17, 19, 20). $G\alpha_{12/13}$-mediated Ang II- or ET-1-induced cardiac fibroblast transformation is essential for cardiac remodeling and heart failure induced by pressure overload (17–20). Moreover, $G\alpha_{12/13}$ are indispensable for cell proliferation (54) and migration (55). G_q/G_{11} alone can couple GPCRs to the rapid activation of RhoA by direct protein-protein interaction with p63RhoGEF independently (56) and, therefore, mediated induction of CTGF and TGF-β1 (57). As discussed above, RhoA could be activated by both $G\alpha_{12/13}$ and $G\alpha_{q/11}$. However, RhoA activation induced by receptor agonists via $G\alpha_{q/11}$ occurs with lower potency than RhoA activation via $G\alpha_{12/13}$ in NIH3T3 fibroblasts (53), suggesting a predominant role of $G\alpha_{12/13}$ for RhoA activation. In line with this, other previous studies have demonstrated that G_q family protein predominantly regulates the pathogenesis of hypertrophy (17, 58, 59) and $G\alpha_{12/13}$ primarily mediates fibrosis (17). The concepts above suggest limited contributions of $G\alpha_{q/11}$ for RhoA activation and subsequent fibrotic response. In the present study, we have shown that $G\alpha_{12/13}$ activation induced by Ang II was attenuated by 11,12-EET. Moreover, silencing $G\alpha_{12/13}$ exerted similar effects of 11,12-EET on alleviating RhoA activation and subsequent fibrotic response. We also detected PLCβ phosphorylation, which represents the major downstream effecter pathway of $G\alpha_{q/11}$ (60). Results showed that PLCβ phosphorylation induced by Ang II was not inhibited by 11,12-EET. Taken together, we identified that 11,12-EET inhibits RhoA activation and subsequent fibrotic response by targeting $G\alpha_{12/13}$.

Inhibition of the RhoA/ROCK/MRTF-A pathway mediated anti-fibrotic effects of EETs

Once AT1R is stimulated, the coupled $G\alpha_{12/13}$ is activated, subsequently activate RhoA by DH/PH domains of RhoGEF, which facilitate the exchange of GDP for GTP (29, 61, 62). Effects of RhoA are mediated by the well-established downstream effectors, ROCKs, which stimulate actin polymerization, liberate MRTF-A from G-actin, and expose a nuclear localization sequence within the actin-binding domain of MRTF-A (63). The above process ultimately activates the myofibroblast-like phenotype in cultured cardiac fibroblasts and enhances the transcription of genes encoding ECM components from cardiac fibroblasts (64). The RhoA/ROCK/MRTF-A pathway, which is the downstream mediator of $G\alpha_{12/13}$, was detected to further elucidate mechanisms of the anti-fibrotic effects of EETs. Results revealed that, besides $G\alpha_{12/13}$ inhibition, CYP2J2 overexpression or EET treatment inhibited the activities of RhoA and ROCK, as well as decreasing MRTF-A nuclear translocation in vivo and in vitro, which indicated that $G\alpha_{12/13}$/RhoA/ROCK/MRTF-A pathway inhibition was involved in the anti-fibrotic effects of EETs. Silencing of $G\alpha_{12/13}$ or RhoA exerts similar effects of 11,12-EET on the inhibition of fibrotic response and MRTF-A nuclear translocation, which further supports the concept that EETs alleviate cardiac fibrotic response by inhibiting the $G\alpha_{12/13}$/RhoA/ROCK/MRTF-A pathway. This mechanism was supported by various other studies because the $G\alpha_{12/13}$/RhoA/ROCK/MRTF-A pathway is pivotal in the pathophysiological process, including mechanical stress fiber formation, tissue fibrosis, cell proliferation, cell migration, and myofibroblast transformation (21–23, 64–67). Moreover, inhibition of the $G\alpha_{12/13}$/RhoA/ROCK/MRTF-A pathway by pharmacological inhibition or gene knockout exerts similar effects of EETs, which alleviate solid organ remodeling including cardiac hypertrophy and fibrosis (17, 18, 24, 68–70) and attenuate transcription of genes encoding ECM components at the molecular level (64, 71). In conclusion, $G\alpha_{12/13}$ inhibition by EETs exerts an anti-fibrotic role by reducing activation of the RhoA/ROCK/MRTF-A pathway.

CONCLUSIONS

Our data indicate that cardiomyocyte-specific expression of CYP2J2 improves EET formation and, therefore, prevents cardiac hypertrophy and fibrosis. EETs attenuate cardiac hypertrophy by acting directly on cardiomyocytes via targeting the PPAR-γ/oxidative stress/SERCA2a/ER stress pathway and promoting interaction of Akt1 and AMPKα2β2γ1 (8, 13, 14). EETs alleviate cardiac fibrosis by acting on diverse cell types. Previous studies have indicated that EETs alleviate cardiac fibrosis by decreasing secretion of pro-fibrotic factors (TIMP1, TGF-β1, and H_2O_2) and pro-inflammatory cytokines (IL-6, IL-1β, and MCP-1) from cardiomyocytes and macrophages, respectively, which results in inhibitory effects on the activation of cardiac fibroblasts (13, 15). This study focuses on the direct effects of EETs on cardiac fibroblasts and indicates that EETs attenuate cardiac fibrosis by inhibiting the fibrotic response of cardiac fibroblasts, including inhibition of cardiac fibroblast proliferation, transformation, migration, and collagen secretion. Mechanistically, the anti-fibrotic effects of EETs are mediated by inhibiting the $G\alpha_{12/13}$/RhoA/ROCK pathway via activating NO/cGMP signaling. This study yields significant insights into the beneficial effects of EETs in cardiac fibroblasts during cardiac fibrosis.

The present study demonstrates that EETs markedly attenuate fibrotic response by reducing activation of cardiac fibroblasts via inhibition of the $G\alpha_{12/13}$/RhoA/ROCK pathway by activating NO/cGMP signaling. The beneficial

effects of EETs on cardiac fibroblasts, however, may involve other mechanisms, which warrant further study in future.⬛

REFERENCES

1. Chen, J., G. C. Shearer, Q. Chen, C. L. Healy, A. J. Beyer, V. B. Nareddy, A. M. Gerdes, W. S. Harris, T. D. O'Connell, and D. Wang. 2011. Omega-3 fatty acids prevent pressure overload-induced cardiac fibrosis through activation of cyclic GMP/protein kinase G signaling in cardiac fibroblasts. *Circulation.* **123:** 584–593.

2. Koitabashi, N., and D. A. Kass. 2011. Reverse remodeling in heart failure–mechanisms and therapeutic opportunities. *Nat. Rev. Cardiol.* **9:** 147–157.

3. Nagpal, V., R. Rai, A. T. Place, S. B. Murphy, S. K. Verma, A. K. Ghosh, and D. E. Vaughan. 2016. MiR-125b is critical for fibroblast-to-myofibroblast transition and cardiac fibrosis. *Circulation.* **133:** 291–301.

4. Sun, M., H. Yu, Y. Zhang, Z. Li, and W. Gao. 2015. MicroRNA-214 mediates isoproterenol-induced proliferation and collagen synthesis in cardiac fibroblasts. *Sci. Rep.* **5:** 18351.

5. Xu, X., X. A. Zhang, and D. W. Wang. 2011. The roles of CYP450 epoxygenases and metabolites, epoxyeicosatrienoic acids, in cardiovascular and malignant diseases. *Adv. Drug Deliv. Rev.* **63:** 597–609.

6. Imig, J. D. 2012. Epoxides and soluble epoxide hydrolase in cardiovascular physiology. *Physiol. Rev.* **92:** 101–130.

7. Fleming, I. 2014. The pharmacology of the cytochrome P450 epoxygenase/soluble epoxide hydrolase axis in the vasculature and cardiovascular disease. *Pharmacol. Rev.* **66:** 1106–1140.

8. Wang, X., L. Ni, L. Yang, Q. Duan, C. Chen, M. L. Edin, D. C. Zeldin, and D. W. Wang. 2014. CYP2J2-derived epoxyeicosatrienoic acids suppress endoplasmic reticulum stress in heart failure. *Mol. Pharmacol.* **85:** 105–115.

9. Ma, B., X. Xiong, C. Chen, H. Li, X. Xu, X. Li, R. Li, G. Chen, R. T. Dackor, D. C. Zeldin, et al. 2013. Cardiac-specific overexpression of CYP2J2 attenuates diabetic cardiomyopathy in male streptozotocin-induced diabetic mice. *Endocrinology.* **154:** 2843–2856.

10. Ai, D., W. Pang, N. Li, M. Xu, P. D. Jones, J. Yang, Y. Zhang, N. Chiamvimonvat, J. Y. Shyy, B. D. Hammock, et al. 2009. Soluble epoxide hydrolase plays an essential role in angiotensin II-induced cardiac hypertrophy. *Proc. Natl. Acad. Sci. USA.* **106:** 564–569.

11. Zhang, L., H. Ding, J. Yan, R. Hui, W. Wang, G. E. Kissling, D. C. Zeldin, and D. W. Wang. 2008. Genetic variation in cytochrome P450 2J2 and soluble epoxide hydrolase and risk of ischemic stroke in a Chinese population. *Pharmacogenet. Genomics.* **18:** 45–51.

12. Spiecker, M., H. Darius, T. Hankeln, M. Soufi, A. M. Sattler, J. R. Schaefer, K. Node, J. Borgel, A. Mugge, K. Lindpaintner, et al. 2004. Risk of coronary artery disease associated with polymorphism of the cytochrome P450 epoxygenase CYP2J2. *Circulation.* **110:** 2132–2136.

13. He, Z., X. Zhang, C. Chen, Z. Wen, S. L. Hoopes, D. C. Zeldin, and D. W. Wang. 2015. Cardiomyocyte-specific expression of CYP2J2 prevents development of cardiac remodelling induced by angiotensin II. *Cardiovasc. Res.* **105:** 304–317.

14. Wang, B., H. Zeng, Z. Wen, C. Chen, and D. W. Wang. 2016. CYP2J2 and its metabolites (epoxyeicosatrienoic acids) attenuate cardiac hypertrophy by activating AMPKalpha2 and enhancing nuclear translocation of Akt1. *Aging Cell.* **15:** 940–952.

15. Yang, L., L. Ni, Q. Duan, X. Wang, C. Chen, S. Chen, S. Chaugai, D. C. Zeldin, J. R. Tang, and D. W. Wang. 2015. CYP epoxygenase 2J2 prevents cardiac fibrosis by suppression of transmission of proinflammation from cardiomyocytes to macrophages. *Prostaglandins Other Lipid Mediat.* **116–117:** 64–75.

16. Behm, D. J., A. Ogbonna, C. Wu, C. L. Burns-Kurtis, and S. A. Douglas. 2009. Epoxyeicosatrienoic acids function as selective, endogenous antagonists of native thromboxane receptors: identification of a novel mechanism of vasodilation. *J. Pharmacol. Exp. Ther.* **328:** 231–239.

17. Nishida, M., Y. Sato, A. Uemura, Y. Narita, H. Tozaki-Saitoh, M. Nakaya, T. Ide, K. Suzuki, K. Inoue, T. Nagao, et al. 2008. P2Y6 receptor-Galpha12/13 signalling in cardiomyocytes triggers pressure overload-induced cardiac fibrosis. *EMBO J.* **27:** 3104–3115.

18. Takefuji, M., A. Wirth, M. Lukasova, S. Takefuji, T. Boettger, T. Braun, T. Althoff, S. Offermanns, and N. Wettschureck. 2012. G(13)-mediated signaling pathway is required for pressure overload-induced cardiac remodeling and heart failure. *Circulation.* **126:** 1972–1982.

19. Fujii, T., N. Onohara, Y. Maruyama, S. Tanabe, H. Kobayashi, M. Fukutomi, Y. Nagamatsu, N. Nishihara, R. Inoue, H. Sumimoto, et al. 2005. Galpha12/13-mediated production of reactive oxygen species is critical for angiotensin receptor-induced NFAT activation in cardiac fibroblasts. *J. Biol. Chem.* **280:** 23041–23047.

20. Nishida, M., N. Onohara, Y. Sato, R. Suda, M. Ogushi, S. Tanabe, R. Inoue, Y. Mori, and H. Kurose. 2007. Galpha12/13-mediated up-regulation of TRPC6 negatively regulates endothelin-1-induced cardiac myofibroblast formation and collagen synthesis through nuclear factor of activated T cells activation. *J. Biol. Chem.* **282:** 23117–23128.

21. Chen, Y., Z. Yang, M. Meng, Y. Zhao, N. Dong, H. Yan, L. Liu, M. Ding, H. B. Peng, and F. Shao. 2009. Cullin mediates degradation of RhoA through evolutionarily conserved BTB adaptors to control actin cytoskeleton structure and cell movement. *Mol. Cell.* **35:** 841–855.

22. Rossman, K. L., C. J. Der, and J. Sondek. 2005. GEF means go: turning on RHO GTPases with guanine nucleotide-exchange factors. *Nat. Rev. Mol. Cell Biol.* **6:** 167–180.

23. Masamune, A., K. Kikuta, M. Satoh, K. Satoh, and T. Shimosegawa. 2003. Rho kinase inhibitors block activation of pancreatic stellate cells. *Br. J. Pharmacol.* **140:** 1292–1302.

24. Rikitake, Y., N. Oyama, C. Y. Wang, K. Noma, M. Satoh, H. H. Kim, and J. K. Liao. 2005. Decreased perivascular fibrosis but not cardiac hypertrophy in ROCK1+/- haploinsufficient mice. *Circulation.* **112:** 2959–2965.

25. Martin, C. B., G. M. Mahon, M. B. Klinger, R. J. Kay, M. Symons, C. J. Der, and I. P. Whitehead. 2001. The thrombin receptor, PAR-1, causes transformation by activation of Rho-mediated signaling pathways. *Oncogene.* **20:** 1953–1963.

26. Gross, G. J., A. Hsu, A. W. Pfeiffer, and K. Nithipatikom. 2013. Roles of endothelial nitric oxide synthase (eNOS) and mitochondrial permeability transition pore (MPTP) in epoxyeicosatrienoic acid (EET)-induced cardioprotection against infarction in intact rat hearts. *J. Mol. Cell. Cardiol.* **59:** 20–29.

27. Jiang, J. G., R. J. Chen, B. Xiao, S. Yang, J. N. Wang, Y. Wang, L. A. Cowart, X. Xiao, D. W. Wang, and Y. Xia. 2007. Regulation of endothelial nitric-oxide synthase activity through phosphorylation in response to epoxyeicosatrienoic acids. *Prostaglandins Other Lipid Mediat.* **82:** 162–174.

28. Wang, H., L. Lin, J. Jiang, Y. Wang, Z. Y. Lu, J. A. Bradbury, F. B. Lih, D. W. Wang, and D. C. Zeldin. 2003. Up-regulation of endothelial nitric-oxide synthase by endothelium-derived hyperpolarizing factor involves mitogen-activated protein kinase and protein kinase C signaling pathways. *J. Pharmacol. Exp. Ther.* **307:** 753–764.

29. Suzuki, H., K. Kimura, H. Shirai, K. Eguchi, S. Higuchi, A. Hinoki, K. Ishimaru, E. Brailoiu, D. N. Dhanasekaran, L. N. Stemmle, et al. 2009. Endothelial nitric oxide synthase inhibits G12/13 and rho-kinase activated by the angiotensin II type-1 receptor: implication in vascular migration. *Arterioscler. Thromb. Vasc. Biol.* **29:** 217–224.

30. Seubert, J., B. Yang, J. A. Bradbury, J. Graves, L. M. Degraff, S. Gabel, R. Gooch, J. Foley, J. Newman, L. Mao, et al. 2004. Enhanced post-ischemic functional recovery in CYP2J2 transgenic hearts involves mitochondrial ATP-sensitive K+ channels and p42/p44 MAPK pathway. *Circ. Res.* **95:** 506–514.

31. Ma, H., H. Gong, Z. Chen, Y. Liang, J. Yuan, G. Zhang, J. Wu, Y. Ye, C. Yang, A. Nakai, et al. 2012. Association of Stat3 with HSF1 plays a critical role in G-CSF-induced cardio-protection against ischemia/reperfusion injury. *J. Mol. Cell. Cardiol.* **52:** 1282–1290.

32. Shioura, K. M., D. L. Geenen, and P. H. Goldspink. 2007. Assessment of cardiac function with the pressure-volume conductance system following myocardial infarction in mice. *Am. J. Physiol. Heart Circ. Physiol.* **293:** H2870–H2877.

33. Dubey, R. K., D. G. Gillespie, Z. Mi, and E. K. Jackson. 1997. Exogenous and endogenous adenosine inhibits fetal calf serum-induced growth of rat cardiac fibroblasts: role of A2B receptors. *Circulation.* **96:** 2656–2666.

34. Askar, S. F., B. O. Bingen, M. J. Schalij, J. Swildens, D. E. Atsma, C. I. Schutte, A. A. de Vries, K. Zeppenfeld, D. L. Ypey, and D. A. Pijnappels. 2013. Similar arrhythmicity in hypertrophic and fibrotic cardiac cultures caused by distinct substrate-specific mechanisms. *Cardiovasc. Res.* **97:** 171–181.

35. Kassiri, Z., V. Defamie, M. Hariri, G. Y. Oudit, S. Anthwal, F. Dawood, P. Liu, and R. Khokha. 2009. Simultaneous transforming growth factor beta-tumor necrosis factor activation and cross-talk cause aberrant remodeling response and myocardial fibrosis in Timp3-deficient heart. *J. Biol. Chem.* **284:** 29893–29904.

36. Odenbach, J., X. Wang, S. Cooper, F. L. Chow, T. Oka, G. Lopaschuk, Z. Kassiri, and C. Fernandez-Patron. 2011. MMP-2 mediates angiotensin II-induced hypertension under the transcriptional control of MMP-7 and TACE. *Hypertension.* **57:** 123–130.

37. Yan-Hong, F., D. Hui, P. Qing, S. Lei, W. Hai-Chang, Z. Wei, and C. Yan-Jie. 2010. Effects of arginine vasopressin on differentiation of cardiac fibroblasts into myofibroblasts. *J. Cardiovasc. Pharmacol.* **55:** 489–495.

38. Amano, M., M. Ito, K. Kimura, Y. Fukata, K. Chihara, T. Nakano, Y. Matsuura, and K. Kaibuchi. 1996. Phosphorylation and activation of myosin by Rho-associated kinase (Rho-kinase). *J. Biol. Chem.* **271:** 20246–20249.

39. Zhao, J., and H. Lei. 2016. Tripartite motif protein 72 regulates the proliferation and migration of rat cardiac fibroblasts via the transforming growth factor-beta signaling pathway. *Cardiology.* **134:** 340–346.

40. Zhang, X., N. Yang, D. Ai, and Y. Zhu. 2015. Systematic metabolomic analysis of eicosanoids after omega-3 polyunsaturated fatty acid supplementation by a highly specific liquid chromatography-tandem mass spectrometry-based method. *J. Proteome Res.* **14:** 1843–1853.

41. Li, L., N. Li, W. Pang, X. Zhang, B. D. Hammock, D. Ai, and Y. Zhu. 2014. Opposite effects of gene deficiency and pharmacological inhibition of soluble epoxide hydrolase on cardiac fibrosis. *PLoS One.* **9:** e94092.

42. Imig, J. D., and B. D. Hammock. 2009. Soluble epoxide hydrolase as a therapeutic target for cardiovascular diseases. *Nat. Rev. Drug Discov.* **8:** 794–805.

43. Spector, A. A. 2009. Arachidonic acid cytochrome P450 epoxygenase pathway. *J. Lipid Res.* **50 (Suppl.):** S52–S56.

44. Brown, R. D., S. K. Ambler, M. D. Mitchell, and C. S. Long. 2005. The cardiac fibroblast: therapeutic target in myocardial remodeling and failure. *Annu. Rev. Pharmacol. Toxicol.* **45:** 657–687.

45. Imig, J. D. 2005. Epoxide hydrolase and epoxygenase metabolites as therapeutic targets for renal diseases. *Am. J. Physiol. Renal Physiol.* **289:** F496–F503.

46. Spector, A. A., X. Fang, G. D. Snyder, and N. L. Weintraub. 2004. Epoxyeicosatrienoic acids (EETs): metabolism and biochemical function. *Prog. Lipid Res.* **43:** 55–90.

47. Hofmann, F. 2005. The biology of cyclic GMP-dependent protein kinases. *J. Biol. Chem.* **280:** 1–4.

48. Rybalkin, S. D., C. Yan, K. E. Bornfeldt, and J. A. Beavo. 2003. Cyclic GMP phosphodiesterases and regulation of smooth muscle function. *Circ. Res.* **93:** 280–291.

49. Chung, H. H., Z. K. Dai, B. N. Wu, J. L. Yeh, C. Y. Chai, K. S. Chu, C. P. Liu, and I. J. Chen. 2010. The xanthine derivative KMUP-1 inhibits models of pulmonary artery hypertension via increased NO and cGMP-dependent inhibition of RhoA/Rho kinase. *Br. J. Pharmacol.* **160:** 971–986.

50. Zhang, L., Y. Cui, B. Geng, X. Zeng, and C. Tang. 2008. 11,12-Epoxyeicosatrienoic acid activates the L-arginine/nitric oxide pathway in human platelets. *Mol. Cell. Biochem.* **308:** 51–56.

51. Kozasa, T., and A. G. Gilman. 1996. Protein kinase C phosphorylates G12 alpha and inhibits its interaction with G beta gamma. *J. Biol. Chem.* **271:** 12562–12567.

52. Balakumar, P., and G. Jagadeesh. 2014. A century old renin-angiotensin system still grows with endless possibilities: AT1 receptor signaling cascades in cardiovascular physiopathology. *Cell. Signal.* **26:** 2147–2160.

53. Vogt, S., R. Grosse, G. Schultz, and S. Offermanns. 2003. Receptor-dependent RhoA activation in G12/G13-deficient cells: genetic evidence for an involvement of Gq/G11. *J. Biol. Chem.* **278:** 28743–28749.

54. Ha, J. H., R. Gomathinayagam, M. Yan, M. Jayaraman, R. Ramesh, and D. N. Dhanasekaran. 2015. Determinant role for the gep oncogenes, Galpha12/13, in ovarian cancer cell proliferation and xenograft tumor growth. *Genes Cancer.* **6:** 356–364.

55. Goulimari, P., T. M. Kitzing, H. Knieling, D. T. Brandt, S. Offermanns, and R. Grosse. 2005. Galpha12/13 is essential for directed cell migration and localized Rho-Dia1 function. *J. Biol. Chem.* **280:** 42242–42251.

56. Lutz, S., A. Freichel-Blomquist, Y. Yang, U. Rumenapp, K. H. Jakobs, M. Schmidt, and T. Wieland. 2005. The guanine nucleotide exchange factor p63RhoGEF, a specific link between Gq/11-coupled receptor signaling and RhoA. *J. Biol. Chem.* **280:** 11134–11139.

57. Ongherth, A., S. Pasch, C. M. Wuertz, K. Nowak, N. Kittana, C. A. Weis, C. Jatho, C. Vettel, M. Tiburcy, K. Toischer, et al. 2015. p63RhoGEF regulates auto- and paracrine signaling in cardiac fibroblasts. *J. Mol. Cell. Cardiol.* **88:** 39–54.

58. Adams, J. W., Y. Sakata, M. G. Davis, V. P. Sah, Y. Wang, S. B. Liggett, K. R. Chien, J. H. Brown, and G. W. Dorn III. 1998. Enhanced Galphaq signaling: a common pathway mediates cardiac hypertrophy and apoptotic heart failure. *Proc. Natl. Acad. Sci. USA.* **95:** 10140–10145.

59. Wettschureck, N., H. Rutten, A. Zywietz, D. Gehring, T. M. Wilkie, J. Chen, K. R. Chien, and S. Offermanns. 2001. Absence of pressure overload induced myocardial hypertrophy after conditional inactivation of Galphaq/Galpha11 in cardiomyocytes. *Nat. Med.* **7:** 1236–1240.

60. Wettschureck, N., and S. Offermanns. 2005. Mammalian G proteins and their cell type specific functions. *Physiol. Rev.* **85:** 1159–1204.

61. Hepler, J. R., and A. G. Gilman. 1992. G proteins. *Trends Biochem. Sci.* **17:** 383–387.

62. Tanaka, S., Y. Fukumoto, K. Nochioka, T. Minami, S. Kudo, N. Shiba, Y. Takai, C. L. Williams, J. K. Liao, and H. Shimokawa. 2013. Statins exert the pleiotropic effects through small GTP-binding protein dissociation stimulator upregulation with a resultant Rac1 degradation. *Arterioscler. Thromb. Vasc. Biol.* **33:** 1591–1600.

63. Ho, C. Y., D. E. Jaalouk, M. K. Vartiainen, and J. Lammerding. 2013. Lamin A/C and emerin regulate MKL1-SRF activity by modulating actin dynamics. *Nature.* **497:** 507–511.

64. Small, E. M., J. E. Thatcher, L. B. Sutherland, H. Kinoshita, R. D. Gerard, J. A. Richardson, J. M. Dimaio, H. Sadek, K. Kuwahara, and E. N. Olson. 2010. Myocardin-related transcription factor-a controls myofibroblast activation and fibrosis in response to myocardial infarction. *Circ. Res.* **107:** 294–304.

65. Iwanciw, D., M. Rehm, M. Porst, and M. Goppelt-Struebe. 2003. Induction of connective tissue growth factor by angiotensin II: integration of signaling pathways. *Arterioscler. Thromb. Vasc. Biol.* **23:** 1782–1787.

66. Kataoka, C., K. Egashira, S. Inoue, M. Takemoto, W. Ni, M. Koyanagi, S. Kitamoto, M. Usui, K. Kaibuchi, H. Shimokawa, et al. 2002. Important role of Rho-kinase in the pathogenesis of cardiovascular inflammation and remodeling induced by long-term blockade of nitric oxide synthesis in rats. *Hypertension.* **39:** 245–250.

67. Velasquez, L. S., L. B. Sutherland, Z. Liu, F. Grinnell, K. E. Kamm, J. W. Schneider, E. N. Olson, and E. M. Small. 2013. Activation of MRTF-A-dependent gene expression with a small molecule promotes myofibroblast differentiation and wound healing. *Proc. Natl. Acad. Sci. USA.* **110:** 16850–16855.

68. Shimizu, Y., K. Dobashi, K. Iizuka, T. Horie, K. Suzuki, H. Tukagoshi, T. Nakazawa, Y. Nakazato, and M. Mori. 2001. Contribution of small GTPase Rho and its target protein rock in a murine model of lung fibrosis. *Am. J. Respir. Crit. Care Med.* **163:** 210–217.

69. Satoh, S., Y. Ueda, M. Koyanagi, T. Kadokami, M. Sugano, Y. Yoshikawa, and N. Makino. 2003. Chronic inhibition of Rho kinase blunts the process of left ventricular hypertrophy leading to cardiac contractile dysfunction in hypertension-induced heart failure. *J. Mol. Cell. Cardiol.* **35:** 59–70.

70. Higashi, M., H. Shimokawa, T. Hattori, J. Hiroki, Y. Mukai, K. Morikawa, T. Ichiki, S. Takahashi, and A. Takeshita. 2003. Long-term inhibition of Rho-kinase suppresses angiotensin II-induced cardiovascular hypertrophy in rats in vivo: effect on endothelial NAD(P)H oxidase system. *Circ. Res.* **93:** 767–775.

71. Zhou, Y., X. Huang, L. Hecker, D. Kurundkar, A. Kurundkar, H. Liu, T. H. Jin, L. Desai, K. Bernard, and V. J. Thannickal. 2013. Inhibition of mechanosensitive signaling in myofibroblasts ameliorates experimental pulmonary fibrosis. *J. Clin. Invest.* **123:** 1096–1108.